A Limited-Scope Probabilistic Risk Assessment Study to Risk-Inform the Design of a Fuel Storage System for Spent Pebble-Filled Dry Casks

Joomyung Lee, Havva Tayfur, Mostafa M. Hamza, Yahya A. Alzahrani 🟢 **and Mihai A. Diaconeasa *** 🟢

Department of Nuclear Engineering, North Carolina State University, Raleigh, NC 27695, USA
* Correspondence: madiacon@ncsu.edu

Abstract: This limited-scope study demonstrates the application of probabilistic risk assessment (PRA) methodologies to a spent fuel storage system for spent pebble-filled dry cask with a focus only on the necessary PRA technical elements sufficient to risk-inform the spent fuel storage system design. A dropping canister scenario in a silo of the spent fuel storage system is analyzed through an initiating event (IE) identification from the Master Logic Diagram (MLD); event sequence analysis (ES) by establishing the event tree; data analysis (DA) for event sequence quantification (ESQ) with uncertainty quantification; mechanistic source term (MST) analysis by using ORIGEN; radiological consequence analysis (RC) by deploying MicroShield, and risk integration (RI) by showing the Frequency-Consequence (F-C) target curve in the emergency area boundary (EAB). Additionally, a sensitivity study is conducted using the ordinary least square (OLS) regression method to assess the impact of variables such as failed pebble numbers, their location in the canister, and building wall thickness. Furthermore, the release categories grouped from the end states in the event tree are verified as safety cases through the F-C curve. This study highlights the implementation of PRA elements in a logical and structured manner, using appropriate methodologies and computational tools, thereby showing how to risk-inform the design of a dry cask system for storing spent pebble-filled fuel.

Keywords: probabilistic risk assessment; spent fuel storage system; spent pebble-filled dry cask; PRA elements; risk quantification

1. Introduction

1.1. Background of the Dry Cask Storage System and Very High-Temperature Gas Reactor

Since the early 1980s, spent nuclear fuel (SNF) has been managed by the dry cask storage system in the nuclear power plant (NPP) site. As the demand for more spaces and longer storage periods increases, many reactor operators start to utilize dry storage as the existing spent fuel storage pool which not only costs more in the form of high operation and maintenance but also produces radioactive waste [1]. After discharge of the fuel from the reactor, the SNF is stored in an on-site water pool to cool the fuel, which intensively generates radioactivity with heat, for a few years until the released radioactivity decays enough to be moved to dry storage. The main goals of the dry storage system operation are (1) cooling of the fuel to maintain the temperature at a controllable level, (2) prevention of the radioactive release by isolating the fuel with shielding and an enclosed cask, and (3) safety in maintenance from accident scenarios. Compared to wet storage, the dry cask storage method is beneficial because of (1) less corrosion of the stored SNF, (2) good mobility, (3) no concern for cooling water management, and (4) no concern for secondary generated radioactive waste [2]. In virtue of the mentioned advantages, the high requirement for utilizing the dry cask storage system is emphasized at the congressional level. According to the congressional research service report for Congress, Senator Dianne

Feinstein kept asking NRC and related institutions to establish regulatory policies for a faster shift process of the SNF to dry cask in March 2011 [3] because the SNF in the on-site water pool might be threatened by an external hazard. In fact, there were no problems with the dry storage in the Fukushima Daiichi accident, while Units 1, 2, and 3 were damaged due to cooling system failures [4]. For these reasons, the importance of the dry cask method as an SNF storage system is enhanced.

There have been several SNF-related Probabilistic Risk Assessment (PRA) research studies conducted to manage the light water reactor (LWR) SNF in dry cask storage safely. In 2007, a pilot PRA study was implemented to provide a guide for assessing and quantifying the risk associated with dry cask storage system operation by examining the feasible events in discharging, transferring, moving, and storing processes [5]. It covered initiating event (IE) identification including internal events and external hazards; potential failure risk due to mechanical, thermal loads, canister, or fuel failure, and radioactive release-related risk with a secondary containment isolation failure. NRC assigned the Idaho National Laboratory (INL) to evaluate the risk significance for the dry cask system operation from the License Amendment Requests (LAR) perspective [6]. Since a high burn-up of the SNF is essential not only for using the fuel economically but also for safe management of the SNF in the dry cask storage, the dry cask was modeled with a thermal load consideration to demonstrate the high burn-up behavior for installation licensing renewals or transportation licensing support [7]. Besides the dry cask storage PRA, the SPF pool PRA research was also performed, and related challenges are listed [8–10]. Previous studies were conducted to evaluate the risks and issue licenses for managing SNF from LWRs, rather than from advanced non-LWR system, such as a very high-temperature gas reactor (VHTR). Despite the anticipated global development of Generation IV nuclear reactor systems, PRA research for SNF management has been confined to the existing LWR domain.

The Generation IV design project aims to develop the next-generation nuclear energy system to be safer in public, more efficient and economical, and a less waste-producing operation [10–12]. The VHTR is a type of proposed next-generation nuclear plant that is a helium-cooled, graphite-moderated, and graphite-reflected reactor with tri-structural isotropic (TRISO)-coated pebble fuel or prismatic block fuel [13]. The VHTR system research plan [14] was initiated to elaborate tasks for fuel and the fuel cycle [15]; materials [16,17]; hydrogen production; computational validation and methodology [18–20], and benchmark project [21]. In China, a high-temperature gas-cooled reactor-pebble bed module 600 (HTR-PM 600) was developed as a commercial version of the HTR-PM, which is a follow-up reactor of the high-temperature gas-cooled reactor-10 (HTR-10) demonstration project [22]. In the United States, as well as the development of VHTR with a small and micro pebble, the advanced reactor demonstration program (ARDP) was launched by INL and Argonne National Laboratory (ANL) with U.S. universities to research and apply advanced computational techniques for system analysis [18], developing the application tool based on thermal-hydraulic simulation codes [19], and coupling codes to validate the experiments [20]. Additionally, from the material management perspective, the Oak Ridge National Laboratory (ORNL) established the material control and counting (MC&A) plan for pebble bed reactors (PBR) to resolve the safeguards and security-related issues [16,17].

Historically, VHTR PRA was performed by similar methods to those used for the LWR, however, in company with the evolution of the coated particle fuel, the VHTR PRA techniques have grown with the evolution of reactor design and licensing issues [23–27]. The licensing modernization project (LMP) established risk-informed and performance-based licensing technical requirements for advanced non-LWRs through the evaluation of a licensing basis event (LBE) and structures, systems, and components (SSC) performance [27–29]. For severe accident progression, source term, and consequence analysis from the LBE and the SSC performance, U.S. NRC plans to improve the capabilities of the existing computational simulation code, including MELCOR, MACCS, and SCALE [30]. Recently, the American Society of Mechanical Engineers/American Nuclear Society (ASME/ANS) joint committee published the PRA standard for non-LWR to announce the PRA technical

requirements and application process [31]. Most of the previous projects and plans deal with VHTR design and license-oriented topics that focus on operating a reactor safely and preventing the LBE. On the other hand, the spent fuel-related tasks are stated only in the nonmandatory appendices in the PRA standard report.

1.2. Research Objective

The objective of this paper is to demonstrate the PRA requirements for a spent pebble bed-filled dry cask in order to contribute to the establishment of the PRA of the operation of a dry cask system for the VHTR. While previous research has explored PRA aspects of SNF management and VHTR design and operation, there have been few PRA studies examining the combination of the dry cask method and the spent TRISO fuel from the VHTR. To achieve this goal, several tasks are implemented, including (1) the application of a verified methodology, (2) identification of PRA technical requirements, and (3) risk quantification through the technical requirement process. This study endeavors to employ existing methodologies from non-LWR PRA and available data from dry cask storage operations to identify critical concerns, potential challenges, and limitations associated with the dry cask storage of spent pebble bed-filled canisters. The proposed workflow of this study will serve as a foundation for future investigations aimed at developing an effective PRA framework for non-LWR fuel storage operations. Details of the methodologies are described in the following section.

This paper delimits the scope by considering two aspects: the accident scope and the PRA element scope. For the accident scope, the cask drop scenario is selected because it is a representative mechanical load-related IE during the handling phase and transfer phases for a "moving" dry cask [5]. From the perspective of analyzing the dry cask's performance in response to mechanical loads, the study examines the structural impact resulting from the accidental drop scenario [32]. The interaction between SNF and storage canister due to impact loading [33,34] are examined by employing a finite element model (FEM). For the PRA elements, the ASME/ANS suggested 18 technical requirements [31], and this paper presents initiating event (IE) analysis, event sequence (ESA), data analysis (DA), event sequence quantification (ESQ), mechanistic source term (MST) analysis, radiological consequence analysis (RC), and risk integration (RI).

In this paper, Section 2 introduces general concepts of PRA elements including methodologies. Section 3 illustrates the workflow and dry cask storage system for the spent pebble bed fuel. In Section 4, a case study is implemented, and the conclusion follows in Section 5.

2. Methodology

In this section, the general PRA technical requirements determined in the research scope are introduced, as well as specific demonstrations as to how the spent pebble fuel-filled dry cask system PRA will be performed in the paper.

2.1. Initiating Event Identification

IE is the first disturbance to a normal operation of the NPP, thus, the IE selection is not only the primary step to accomplish the accurate and complete PRA model [35] but also to determine the analysis scope. The advanced non-LWR PRA standard suggests a plant or design-specified systematic approach to ascertain IEs, such as master logic diagram (MLD), failure modes and effort analysis (FMEA), heat balance fault tree (HBFT), or hazard and operability analysis (HAZOP) as a process hazards analysis (PHA) [27,31]. In this paper, the methods for IE identification are briefly introduced and compared, with the most appropriate being employed for the pebble bed-filled dry cask PRA.

- Master Logic Diagram

MLD is a formal logical technique based on a top-down approach to identify the IEs. It decomposes the influential factors from the final consequence, which corresponds to the top event represented by "significant release of radioactive material" until the IEs are identified, and depicts the informative flow about the causes and effects of the risk metrics in a form of

a logical block diagram [36,37]. Thanks to the simple formulation of the MLD, the IEs with related event categories are comprehensively disclosed at the system level when collected knowledge and system/component information are provided, despite the fact that the MLD is dependent on the given information status. Therefore, the MLD methodology has been used in a wide range of research, such as the iodine–sulfur (IS) process [38], chemical installations [37], or NPP facilities [36,39].

- Heat Balance Fault Tree

HBFT aims to identify the IE by detecting a deviation from the thermal balance in the system [27]. Since the HBFT is a fault tree combined with technical considerations for heat/energy balance, it is useful to notice where and why the heat/energy imbalance occurs by tracking the cause and effect. Similar to the MLD, the HBFT is built based on a top-down deductive approach with the top event of "occurrence of heat imbalance due to IE" instead of "radioactive release" [40]. On the contrary, compared to the MLD, the HBFT is a methodology to be specifically applied to the NPP system rather than a generally applicable methodology because the NPP retains a steady state in normal operation from the thermal equilibrium perspective through the heat transport over the multiple connected systems including a reactor, a coolant system, and a heat exchange system [40,41].

- Failure Mode and Effects Analysis

FMEA is a risk assessment methodology to detect and reduce or prevent potential error sources in systems. Through the system analysis and failure analysis by focusing on a single equipment or component, the potential root causes with their effects are determined. In other words, the FMEA is a bottom-up inductive process to evaluate the vulnerability of the system. For IE identification, it is employed to assure how specific components can influence the performance of other components, subsystems, and the main systems [31]. The advantage that the impact of the failure is qualitatively analyzed with detailed descriptions enables the FMEA to have been used and improved in techniques in various industries [42]: digital instrumentation and control (I&C) system analysis for nuclear reactor [43,44]; tritium-breeding test blanket module design for fusion reactor [45]; medical radiotherapy research [46,47]; supply chain management [48], and vehicle recall investigation [49]. However, if the object system is complicated or the demonstration of failure mode contains many details, the number of FMEA tasks increases.

- Hazard and Operability Analysis

HAZOP is one of the PHA techniques to identify causes and consequences of potential hazards and operability by examining departure from normal conditions or process variables. Based on the expertise and professional experiences, the HAZOP analysis team divides the system into several sections, which are called HAZOP nodes, according to the inherited features of the nodes or team-defined principles to evaluate the safety-significant incidents [50]. As it is also a bottom-to-top approach methodology, the tasks to define parameters, deviations, cause and effect, and preventive or mitigative action recommendations would be time-consuming and challenging when the system is complicated [27]. From the PRA application perspective, the HAZOP has been used to figure out the IEs or IE groups for the NPP reactor system [27,51–54].

Table 1 summarizes the features of the introduced methodologies. In this paper, as shown in Figure 1, the MLD is used to identify the IEs by the following steps: (1) the final objective determination, (2) source identification, (3) safety barrier or related SSC identification, (4) safety function challenges or the SSC failure identification, (4) failure mode identification, and (5) IE identification. Additionally, steps 3 and 4 are repeated when there are sub-safety systems or sub-safety functions in the system domain. The MLD applied to the spent pebble fuel-filled dry cask PRA is illustrated in the case study section.

Table 1. Comparison of Methodologies for Initiating Event Identification.

	Approach	Features
Master Logic Diagram	Top-down	- Simple and comprehensive - Depicts the cause and effect in general - Challenges in identifying all event types
Heat Balance Fault Tree		- Able to identify the cause and effect due to specific factors - Deductive fault tree analysis procedure - Nuclear power plant applicable method
Failure Mode and Effects Analysis	Bottom-up	- Well organized to understand the impact of the failure - Not friendly for a complicated system - Time-consuming tasks depending on the level of detail
Hazard and Operability Analysis		- Considers various factors - Not applicable to complex systems and time-consuming tasks to identify potential hazards and operability
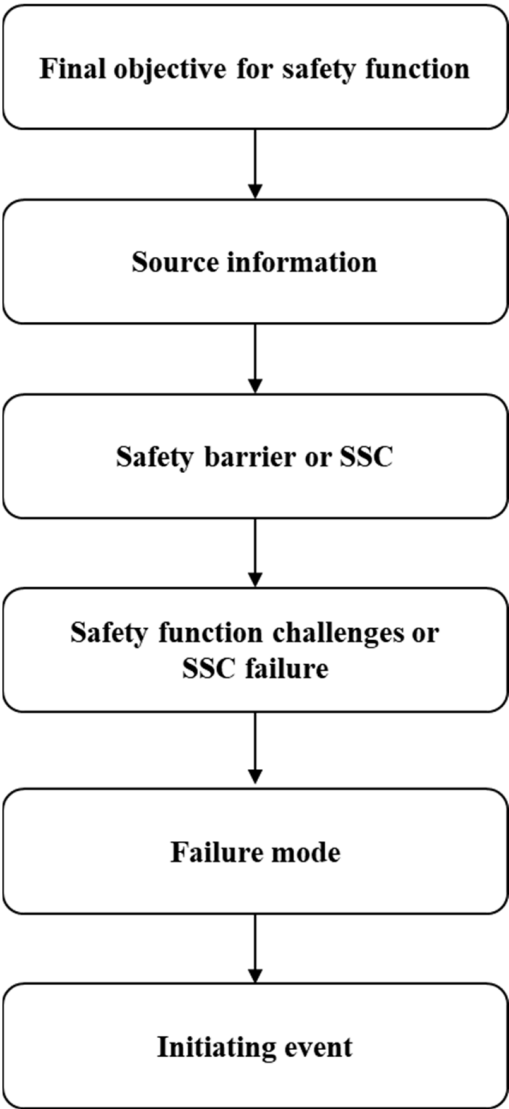
Figure 1. Master Logic Diagram Approach.

2.2. Event Sequence Analysis

The purpose of ESA is to delineate the transient or accident scenarios through timely ordered and consecutively enumerated events based on operator actions and system responses. The ESA provides accident progression represented by the discrete intermediate events that depend on the plant-, design-, and site-specific information from the IEs until the established end states, including core damage or radioactive release [31]. It demonstrates how the incidents are expanded or resolved from the IE by safety function challenges, SSC responses, and preventive or mitigative actions. An event tree (ET) is a representative PRA tool used to illustrate the ES analysis. Figure 2 shows the event sequence modeling framework revised from [27].

Initiating Event	**SSC Responses**	**Reactor and Plant Responses**	**End State**
— Plant operating states — IE from IE identification methodologies	— Safety function challenges — Operator actions	— Dynamic responses by cumulative effects — Failure mode — Operator actions	— Safe stable end-state — Plant damage state — Release categories with mechanistic source terms
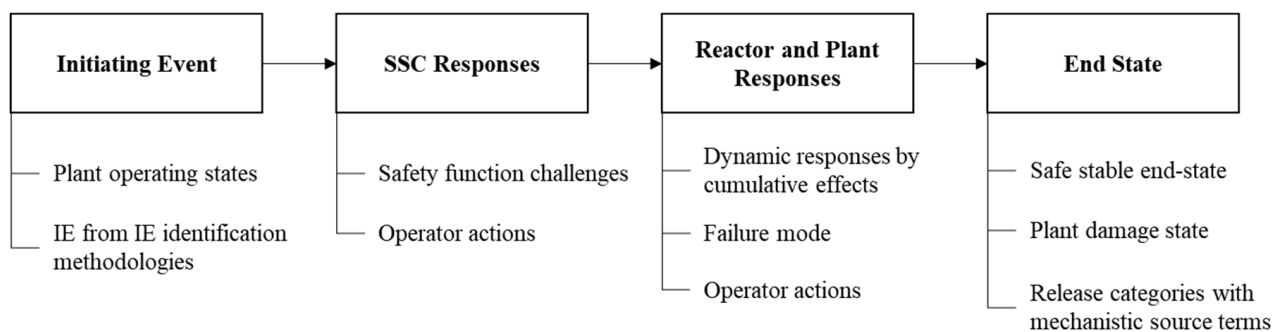
Figure 2. Event Sequence Modeling Framework.

2.3. Data Analysis

DA aims to estimate parameter data with consideration of plant- or system-specific evidence. For obtaining intermediate event probability on the ESA, the following are considered (1) analysis of risk-significant failure mode with associated SSCs or grouped components, (2) common cause failure (CCF) parameter, and (3) equipment maintenance, repair, and recovery-related data [31].

2.4. Event Sequence Quantification

ESQ indicates calculations of the frequency of the specific accident sequences based on the IE frequency and the failure probabilities of the relevant safety functions from the DA process. The objective of ESQ is achieved with (1) a proper computational model required to integrate individual PRA models, (2) solutions for functional and human dependencies, and (3) uncertainty analysis in the quantification process [31].

2.5. Mechanistic Source Term Analysis

MST is defined as the fission product release, led by fuel damage resulting from a particular accident scenario, that the best-estimate model simulates the temporal radionuclide transport in terms of physical and chemical processes [55]. To quantify the source term, the source term characteristics should be determined by consideration of not only released radionuclide transport-related phenomena, such as deposition, condensation, resuspension, and so on, but also system-related information including fuel form, safety engineering system operation states, and component states [56].

2.6. Radiological Consequence Analysis

RC analysis quantifies the consequences of an accident that consists of public health impacts and economic impacts. The health impacts of dose populations are fatalities, injuries, and cancer risk, meanwhile, the economic impacts include evacuation, relocation, and recovery for damaged or contaminated assets costs. Therefore, in addition to the MST analysis data, it is required to model the atmospheric transport and dispersion and obtain site-specific data, such as meteorology data, protective action, and emergency plans for the RC analysis [30].

2.7. Risk Integration

The main objective of the RI is to demonstrate risk-significance criteria with the associated uncertainties of the event sequences. To estimate the risk importance, several risk metrics are suggested and measured for expressing risk based on relative and absolute risk significance [57]. The absolute risk metrics are represented by core damage frequency (CDF), large early release frequency (LERF), or Birnbaum Importance, whereas, for ranking the risk order or establishing the regulations, relative risk measures, including Fussell–Vesely, Risk Achievement, or Risk Achievement Worth, can be used [58]. Depending on the ultimate goal of the PRA performance, decision makers or risk takers would decide the proper risk significance or risk metrics [59].

3. Pebble Fuel-Filled Dry Cask PRA

This section demonstrates the workflow and information flow to achieve the objective of each PRA element and introduces the spent fuel storage system (SFSS) for the HTR-PM as a case study target system. Based on the aforementioned PRA elements, the workflow is established for this study. Although the study concentrates on specific scopes of the PRA elements, the workflow can be extended to cover the full scope of each element for future endeavors. Hence, the introduction of the general non-LWR PRA technical requirements in the previous section will provide a foundation for future applications.

3.1. Workflow

Figure 3 demonstrates the workflow for each PRA element to deliver the information to the next PRA element step.

(1)   Based on the PRA documents including PRA standard, PRA-related reports, and licensing requirements, various data and information are collected and refined to be used as materials for each PRA element or PRA analysis tool. For example, technical information from the pilot PRA study for a dry cask storage system [5] provides safety function-related information to establish the MLD for IE identification.
(2)   From the technical information, the MLD enables to identify the IEs by presenting the causes and effects of the influential failure factors from the final consequences.
(3)   Safety function/system information is utilized from the PRA documents to determine the event sequence that maneuvers the event scenario from the IE onto the end states.
(4)   Same as in the previous steps, the PRA documents are referred to extract and estimate the failure probability of the determined event sequences.
(5)   ESQ is implemented by the Phoenix Architect with the event tree from the ESA and the assumed probability from the DA processes. In this study, CAFTA, PRAQuant, and UNCERT modules are used to develop the fault tree/event tree, quantify the event tree sequences, and perform the uncertainty analysis, respectively.
(6)   For MST analysis, pebble fuel data and release fraction information from the PRA documents are used to tabulate the fuel inventory data for the consequence analysis. ORGIEN 2.2. is used to calculate the nuclide composition and activity of fuel.
(7)   The RCA is performed to simulate the transport of the radioactive nuclides from the source established in the MST analysis according to the release categories by deploying the MicroShield.
(8)   Finally, the risk is evaluated with consideration of frequency and consequence in accordance with the release categories.

Details of each step are demonstrated in the case study section.

3.2. System Description

3.2.1. TRISO Particle and Canister

The TRISO-coated particle fuel is composed of an oxide of uranium and mixtures of carbide and oxides and is encompassed by multiple layers to be safely used in the pebble bed reactor. The multi-layered fuel sphere includes ^{235}U-enriched UO_2 or UCO kernel that

is encapsulated by (1) porous graphite buffer for excellent integrity and conductivity of the particle, (2) inner pyro-carbon (IPyC) to hold non-metal fission products (FPs), (3) silicon carbide (SiC) for retention of metal FPs, and (4) outer pyro-carbon (OPyC) as the last barrier for FP release and the protector for SiC layer [26,60–62]. Figure 4 illustrates the structure of the TRISO kernel with dimension information [63]. A fuel pebble is typically 60 mm in diameter and consists of randomly distributed 8000 to 18,000 fuel particles embedded in the graphite mix [64].
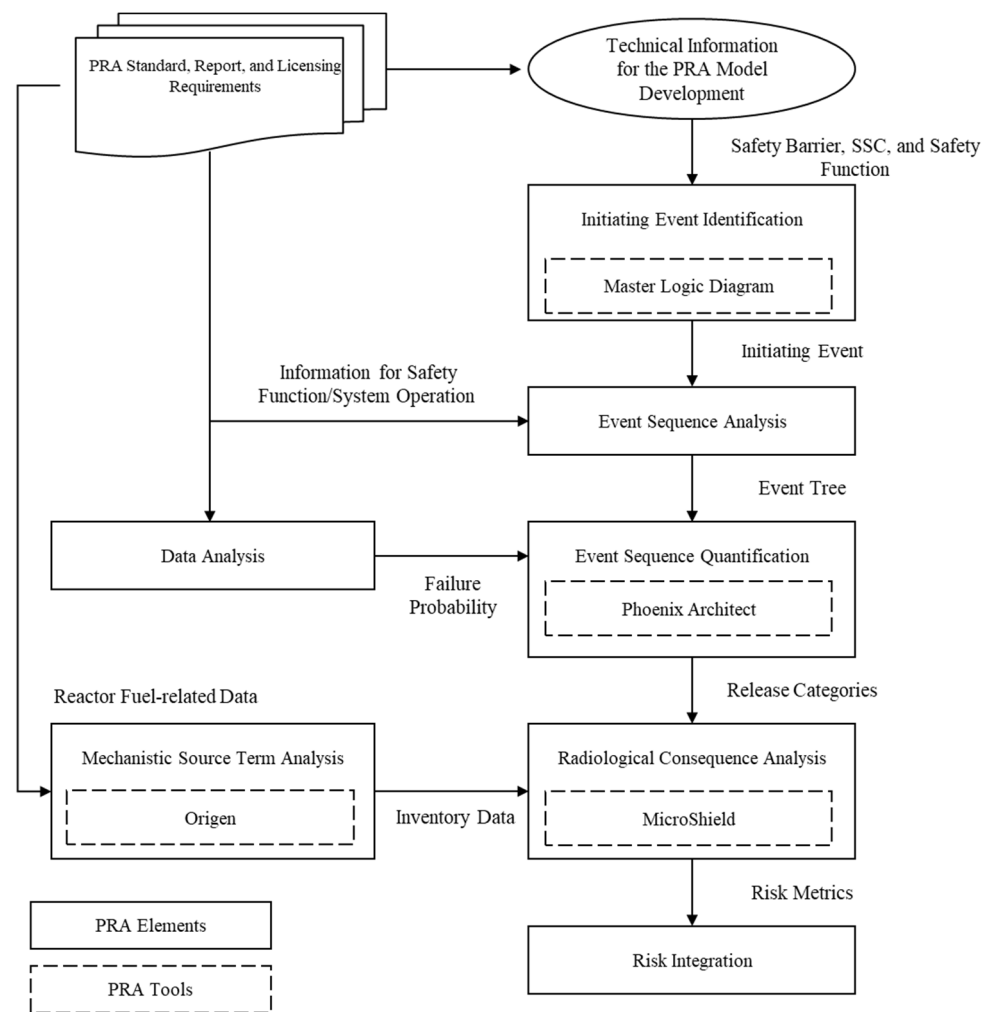

Figure 3. Workflow for Pebble Bed-filled Dry Cask PRA Study.
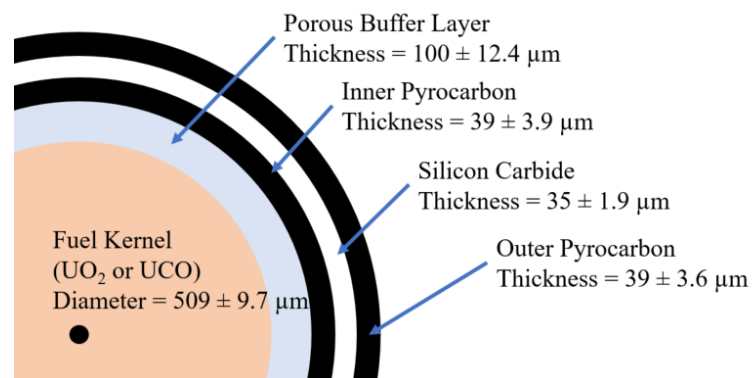

Figure 4. TRISO Kernel Structure.

A canister is a cylindrical stainless-steel structure to accommodate spent fuel elements. In the case of HTR-PM, a canister is 1.74 m in diameter, 4.18 m in height, and 20 mm in thickness to store about 40,000 spent fuel pebbles [65]. Due to the thin thickness, the canister's radiation shielding is vulnerable. Therefore, the spent fuel storage system includes radiation shielding functions when the canisters are transferred, hoisted, and loaded through the conveying and loading system.

3.2.2. Dry Cask Storage System

SFSS for the HTR-PM is a system to transfer the SNF from the reactor to the canister safely through the fuel handling system (FHS) and spent fuel conveying and loading system (SFCLS) and places the spent pebble bed-filled canister in the storage well. The functions of the SFCLS are as follows [66–68]:

- classifying fuel elements into the serviceable fuel element, the spent fuel element, and the graphite element by the direction converter with a burn-up device and retriever device,
- loading the classified elements into the cask or returning them back to the reactor core through the FHS,
- welding the full-filled canister by automatic machine,
- safely stacking the canisters (up to five) into a silo in the storage well by the crane and the hoister,
- and self-cleaning the pipelines by using blowers and iodine/dust filters.

  There are several techniques for the operation of the SFSS with SFCLS:

- Safe stacking: A buffer seat at the bottom of the well protects the canister from dropping accident by structure or mechanistic failure. There are guiding rails and rail seats to load the canisters smoothly.
- Residual heat removal: Three cooling modes are operated in the SFSS to remove decay heat from the pebbles: closed loop active mode, open loop active mode, and open loop passive mode. Table 2 and Figure 5 demonstrate the details of the cooling modes. As Figure 5 shows below, the cold inlet air flows between the wall and barrel, then the air flows upward between the barrel and canister to the outlet pipe.
- Radiation shielding: Besides graphite mix within a fuel pebble, a 304 L stainless steel canister and concrete wall ensure the prevention of radioactive release to the environment.

Table 2. Residual Heat Removal Function in the Spent Fuel Storage System.

	Heat Exchanger	Blower	Feature
Closed Loop Active Cooling Mode	Yes	Yes	• Decrease the corrosion speed of the metal material due to dry air flow
Open Loop Active Cooling Mode	No	Yes	• Wet air flow affects corrosion of the metal material • Used when the heat exchanger is failed or under maintenance
Open Loop Passive Cooling Mode	No	No	• Rely on natural convection only • Used when the blowers fail at the same time

The SFSS is carried out for a buffer storage region in which the full-filled canisters are saved for the first three years because of a large amount of decay heat. Therefore, to maintain the storage temperature below a safe temperature, an independent ventilation system for the residual heat removal system mentioned above is operated. Additionally, since the outlet flow used for the open loop cooling mode is connected to the environ-

ment [67], the filtered ventilation of the heating, ventilation, and air conditioning (HVAC) system is essential to minimize the impact due to radiation release. To define the MLD for IE identification, the safety functions should be investigated.
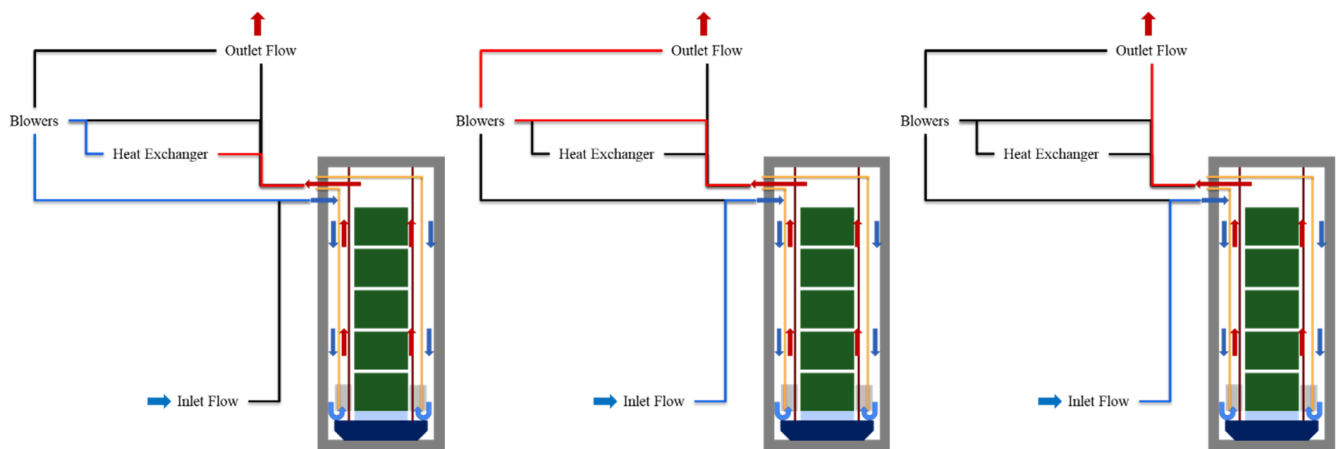
Figure 5. Cooling Modes for the Spent Fuel Storage System ((**Left**): Closed Loop Active Mode, (**Middle**): Open Loop Active Mode, (**Right**): Open Loop Passive Mode).

4. Case Study

A case study is implemented in this section, and each sub-section demonstrates how the PRA techniques are applied to the pebble fuel-filled dry cask PRA thoroughly to achieve its objective with assumptions and utilization of the PRA tools.

### 4.1. Event Description and Case Study Assumptions

To perform the PRA elements step by step, an event scenario is postulated from the canister drop at the silo of the SFSS. Due to the impact of the canister drop, the canister or spent pebbles in it or both is/are damaged. Therefore, the radioactive material can be released depending on the HVAC system operation status. The following are case study assumptions.

✓ Assumptions for IE identification and ESA

(1) There is no SFCLS operation failure or storage building damage during conveying the spent fuels from the FHS to the canister.

(2) There is no residual heat transfer failure caused by low-quality pebble geometry, canister defect, or SFSS cooling mode failure.

(3) There is no concrete wall (silo well) damage while the canister drops.

(4) The fuel particle coating and the graphite mixture in the pebble are not considered as the separated safety barrier for TRISO fuel failure. As mentioned above, the fuel kernel is protected by pyro-carbon layers with silicon carbide and core graphite in the pebble, however, radionuclide release happens when the TRISO is damaged.

(5) Due to improper crane movement, a canister vertically falls onto the concrete floor in the silo. The drop height is varied: 30 m, 25 m, 20 m, 15 m, and 10 m drop height.

(6) It is assumed that the HVAC system is identical to the HVAC system of the secondary containment isolation system for a dry cask storage system from the NUREG-1864 [5]. Therefore, HVAC failure leads to radioactive release directly into the environment bypassing the containment or building.

✓ Assumptions for DA and ESQ

(1) It is assumed that the HVAC system is identical with the HVAC system of the secondary containment isolation system for a dry cask storage system from the NUREG-1864 [5].

(2)   Failure probability due to the impact of the canister drop is assumed by linear interpolation based on given data from [5,69]. Since the failure probability is assumed because of a lack of information, its distribution is induced by the Jeffreys noninformative prior to minimize the influence of the prior input and maximize the influence of the likelihood function [70].

✓ Assumptions for MST

(1)   The reactor operates in a steady-state mode, where the neutron flux and power level are constant over time. This assumption simplifies the calculations by allowing the use of averaged parameters and eliminates the need for time-dependent calculations.

(2)   The fuel is homogeneous and well-mixed, and the temperature distribution is uniform throughout the fuel. This assumption simplifies the modeling of fuel behavior and allows for a more direct calculation of the isotopic composition of the fuel.

(3)   Each pebble does not move during operation, so the geometry of the fuel at the beginning of the cycle remains constant over time. This assumption simplifies the modeling of fuel behavior and allows for a more efficient calculation of the isotopic composition of the fuel.

(4)   The fuel resident time in the reactor is assumed to be 3 years at full power.

✓ Assumptions for RCA and RI

(1)   The 1 MeV energy level is used as the representative energy level for the modeling and analysis of fission product behavior. The behavior of fission products during undesired release to the environment can be complex and is influenced by several factors such as their physical and chemical properties, release characteristics, atmospheric and meteorological conditions, and energy levels. However, to simplify modeling and analysis of dry cask storage system failure, a single energy level is assumed for all fission products. This assumption allows for a more efficient analysis of fission product transport, retention, and release in the event of dry cask storage system accidents. Therefore, selecting 1 MeV allows for the modeling and analysis of fission product behavior to be simplified, as it provides a suitable approximation for many fission products. However, it should be noted that this assumption may not accurately represent the behavior of all fission products in all scenarios, and more detailed modeling might be necessary to investigate in future work. The use of a 1 MeV energy is discussed in relation to fission product transport and deposition, as well as radiological consequences [71–73].

(2)   The release fractions of fission products during the accident are similar to the release fractions used for the LWR spent nuclear fuel. The release fractions used in this study was obtained from NUREG/CR-4982 and NUREG/CR 6451 [74,75].

(3)   There are two concrete walls as the external safety barriers: an inside wall and an outside wall. The inside wall indicates the wall of a silo well and the outside wall is the storage building wall.

(4)   The failed pebble is located at the bottom-center of the canister. For the sensitivity analysis, the pebble number and the failed pebbles' locations are varied.

(5)   The dose point, which is equivalent to the location of the detector, for the absorbed dose rate or exposure rate, is located at 5 km from the source. The 5 km distance is assumed as the exclusion area boundary (EAB) for an advanced reactor [76]. Additionally, for the sensitivity study, another dose point is 10 m from the source which is the vicinity of the storage building.

4.2. Initiating Event Identification by Using MLD

To initiate the PRA analysis, as mentioned above, the MLD is established for identifying IEs of the SFSS operation for the spent pebble bed management. Based on the approach shown in Figure 1, the MLD approach is formulated by considering safety barriers and safety functions which are related to either SFSS operation or spent pebble bed fuel. There are three safety barriers and two main safety challenges: TRISO, canister, and concrete well of the SFSS, and radioactive material release control and heat removal control. Since the heat transfer from the spherical pebbles is dominated by convection, the pebble geometry condition is critical for residual heat removal led by cooling modes [77,78]. Figures 6 and 7 show the MLD approach and MLD of the case study for IE identification, respectively. Among various basic IEs, the canister drop is selected as the IE in accordance with the research scope.
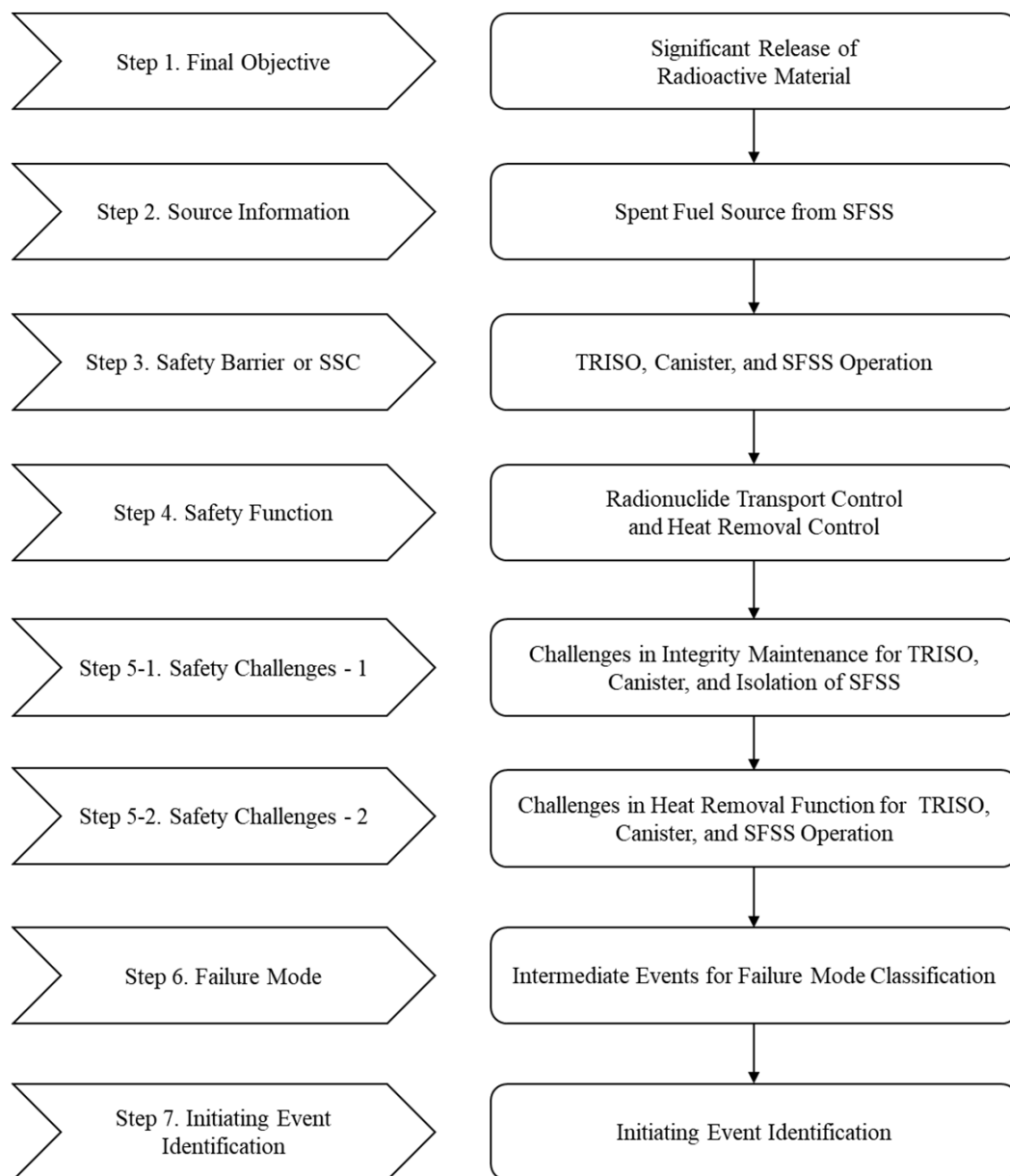
Figure 6. Master Logic Diagram Establishment Approach for the Pebble Bed-Filled Dry Cask PRA.
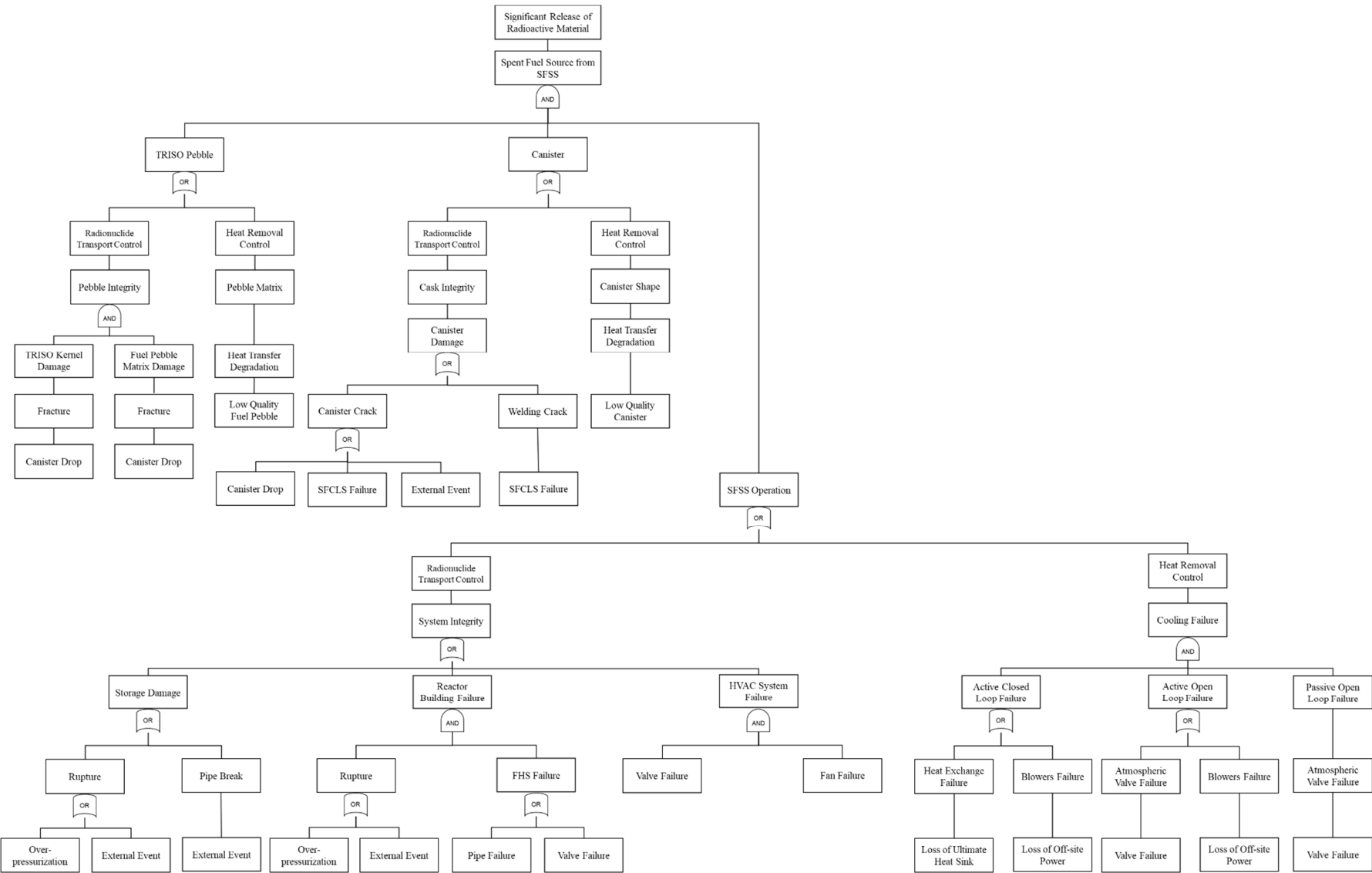
Figure 7. Master Logic Diagram for Spent Fuel Storage System PRA—Event Sequence Analysis for Event Tree Setup.

Event tree is a logical model to describe the event sequences step by step from the IE to the end states for risk analysis. Based on the aforementioned assumptions and safety challenges from the MLD, the event progression is demonstrated by a form of the intermediate events until the determination of the feasible radioactive material release modes. As we can see in Figure 8, only the integrity failure of the pebble bed, canister integrity failure, and HVAC system failure are considered in this case study. The following end states of the event tree are grouped as release categories such as:

- "OK" refers to the no potential risk of release from the SFSS.
- "Direct Exposure" (DE) indicates the event progression that some spent pebbles have failed, but the dry cask is intact. Additionally, the HVAC system operation failure is not considered which means the isolation of the storage is successful.
- "Noble Gas" (NG) is an end state where the release of radionuclide passes through the filtration path of the HVAC system. Since successful HVAC operation enables the filter to retain the radionuclides except the noble gas, only the noble gases, such as Kr and Xe, are released into the environment.
- "Radionuclide Release" (RR) indicates the end state that radioactive material is released to the environment directly without filtration due to HVAC operation failure.
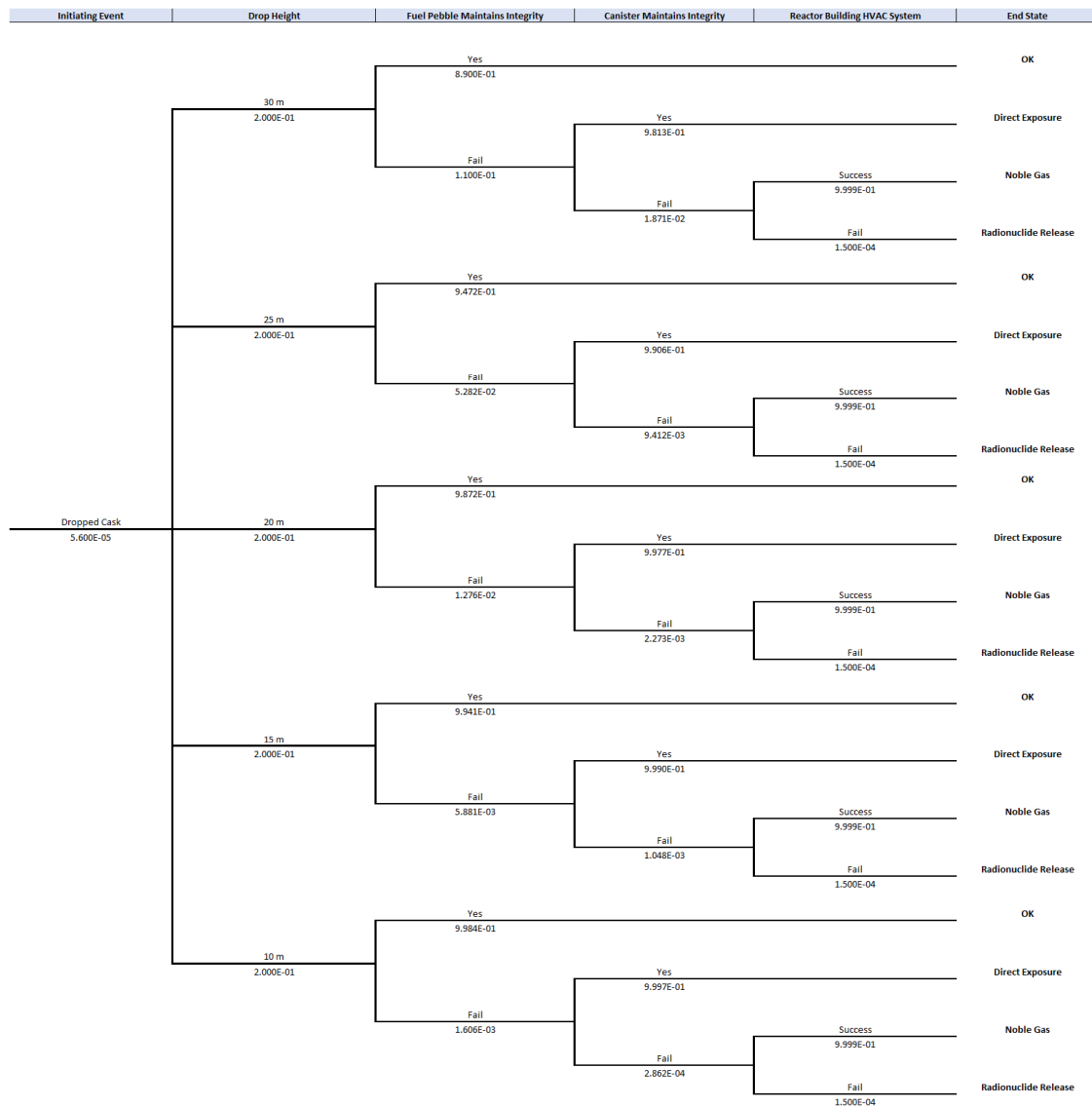
Figure 8. Event Tree for the Case Study (In this work we adopt the "E" notation, which is used to represent "times ten raised to the power of" in the scientific notation).

4.3. Data Analysis for Failure Probability

From the given information and data, the failure frequency/probabilities of the IE and intermediate events are estimated.

- IE frequency is a heuristic frequency given from the dropped transfer cask investigation in the United States [5].
- Canister failure probability is given and estimated by linear interpolation from [5].
- Pebble failure probability at 30 m is given from the dynamic analysis and validation experiment [34]. The failure probabilities with dropping height are assumed with the same proportion of canister failure probabilities.
- HVAC failure probability is given from [5].
- The distributions and parameters for the data are given according to the constrained noninformative distribution (CNID) [69]. For the uncertainty quantification, the initiating event and the other failure probabilities are gamma distribution and beta distribution, respectively [70].
- To maintain the uncertainty magnitude of event sequences, the error factors are consistent from the IE to HVAC failure probability. The error factor is defined as the 95th percentile divided by the median (50th percentile).
- Based on the same error factors, alpha and beta are determined by the equations:

$$\lambda_{IE} = \frac{\alpha_\gamma}{\beta_\gamma}$$

where λ_{IE} refers to the frequency of *IE*. α_γ and β_γ indicate alpha and beta parameters for gamma distribution, respectively. For determining alpha (α_β) and beta (β_β) parameters for beta distribution, the linearly interpolated failure probability (λ_{FP}) is used:

$$\lambda_{FP} = \frac{\alpha_\beta}{\alpha_\beta + \beta_\beta}$$

- To quantify the uncertainties along the event sequences, variances for gamma distribution (Var_γ) and beta distribution (Var_β) are calculated:

$$Var_\gamma = \frac{\alpha_\gamma}{\beta_\gamma{}^2}$$

$$Var_\beta = \frac{\alpha_\beta \beta_\beta}{\left(\alpha_\beta + \beta_\beta\right)^2 \left(\alpha_\beta + \beta_\beta + 1\right)}$$

The calculated probability and parameters are shown in Table 3.

4.4. Event Sequence Quantification by Using Phoenix Architect

For this paper, the Phoenix Architect modular tools are utilized to quantify the event sequence and corresponding uncertainties. The frequency of the end states is calculated through the PRA Quant module by analyzing the event tree and master fault tree developed by the CAFTA module. For the uncertainty quantification in each sequence, the UNCERT module is used with the database established in the PRA Quant module and a 10,000 Monte Carlo sampling size. Tables 4 and 5 show the quantified frequency and uncertainties for the event sequence/release categories, respectively. In this paper, a sample size of 10,000 is selected as a reasonable balance between computational cost and output from the UNCERT module. The mean frequency converges to a point value as the sample size increases, but beyond certain sample sizes, it is not guaranteed that a larger sample size will be closer to the real value due to the randomness of Monte Carlo methods.

4.5. Mechanistic Source Term Analysis by Using ORIGEN

The design characteristics of a high-temperature gas-cooled reactor (HTGR) allow for high thermal efficiency, resulting in the extraction of more energy from the fuel. In this study, an HTGR with a thermal power of 250 MWth was modeled using ORIGEN 2.2 for depletion calculation. The main input parameters are shown in Table 6. The fuel element is spherical with a diameter of 60 mm and contains approximately 12,000 TRISO particles. The TRISO particles are evenly distributed within a graphite matrix that has a diameter of 50 mm. The spherical fuel zone is surrounded by a fuel-free zone made of pure graphite for mechanical and chemical protection. Each TRISO particle comprises a UO_2 kernel with a diameter of 0.5 mm and three additional layers of PyC and SiC. The heavy metal contained in each spherical fuel element is approximately 7.0 g. The fuel element is designed to have an average burn-up rate of 90 GWd/tU, with a maximum fuel burn-up not exceeding 100 GWd/tU.

Table 3. Data Analysis Results for Event Sequence Quantification.

		Frequency/Probability	Distribution	Alpha	Beta	Error Factor	Variance
IE Frequency		5.60×10^{-5}	gamma	5.00×10^{-1}	8.93×10^3	8.44	6.27×10^{-9}
Canister Failure Probability with Dropping Height (m)	30	1.87×10^{-2}	beta	4.87×10^{-1}	2.56×10^1	8.44	6.79×10^{-4}
	25	9.41×10^{-3}	beta	4.94×10^{-1}	5.20×10^1	8.44	1.74×10^{-4}
	20	2.27×10^{-3}	beta	4.99×10^{-1}	2.19×10^2	8.44	1.03×10^{-5}
	15	1.05×10^{-3}	beta	5.00×10^{-1}	4.76×10^2	8.44	2.19×10^{-6}
	10	2.86×10^{-4}	beta	5.00×10^{-1}	1.75×10^3	8.44	1.64×10^{-7}
Pebble Failure Probability with Dropping Height (m)	30	1.10×10^{-1}	beta	4.18×10^{-1}	3.38	8.44	2.04×10^{-2}
	25	5.28×10^{-2}	beta	4.63×10^{-1}	8.30	8.44	5.13×10^{-3}
	20	1.28×10^{-2}	beta	4.92×10^{-1}	3.80×10^1	8.44	3.18×10^{-4}
	15	5.88×10^{-3}	beta	4.96×10^{-1}	8.38×10^1	8.44	6.85×10^{-5}
	10	1.61×10^{-3}	beta	4.99×10^{-1}	3.10×10^2	8.44	5.15×10^{-6}
HVAC Failure Probability		1.50×10^{-4}	beta	5.00×10^{-1}	3.33×10^3	8.44	4.50×10^{-8}

Table 4. Event Sequence Quantification for Sequence Numbers and Groups.

Sequence Number	Frequency	Sequence Number/Group	Frequency
1	9.968×10^{-6}	13	1.113×10^{-5}
2	1.209×10^{-6}	14	6.580×10^{-8}
3	2.304×10^{-8}	15	6.901×10^{-11}
4	3.457×10^{-12}	16	1.035×10^{-14}
5	1.061×10^{-5}	17	1.118×10^{-5}
6	5.860×10^{-7}	18	1.799×10^{-8}
7	5.567×10^{-9}	19	5.149×10^{-12}
8	8.352×10^{-13}	20	7.725×10^{-16}
9	1.106×10^{-5}	OK	5.395×10^{-5}
10	1.425×10^{-7}	Direct Exposure	2.021×10^{-6}
11	3.246×10^{-10}	Noble Gas	2.901×10^{-8}
12	4.870×10^{-14}	Radionuclide Release	4.352×10^{-12}

Table 5. Uncertainty Quantification Results from the Monte Carlo Sampling.

Sequence Number or Sequence Group	Mean Frequency	Uncertainty (10,000 Monte Carlo Samples)		
		5th Percentile	Median	95th Percentile
1	9.904×10^{-6}	4.230×10^{-8}	4.608×10^{-6}	3.776×10^{-5}
2	1.227×10^{-6}	1.283×10^{-10}	1.475×10^{-7}	6.134×10^{-6}
3	2.269×10^{-8}	2.138×10^{-13}	7.440×10^{-10}	9.862×10^{-8}
4	3.486×10^{-12}	3.697×10^{-18}	3.472×10^{-14}	1.087×10^{-11}
5	1.108×10^{-5}	4.173×10^{-8}	5.074×10^{-6}	4.180×10^{-5}
6	6.071×10^{-7}	9.754×10^{-11}	7.292×10^{-8}	2.838×10^{-6}
7	6.037×10^{-9}	7.098×10^{-14}	2.110×10^{-10}	2.657×10^{-8}
8	8.259×10^{-13}	1.311×10^{-18}	8.864×10^{-15}	2.666×10^{-12}
9	1.119×10^{-5}	4.519×10^{-8}	4.954×10^{-6}	4.249×10^{-5}
10	1.441×10^{-7}	2.748×10^{-11}	1.764×10^{-8}	6.921×10^{-7}
11	3.074×10^{-10}	5.343×10^{-15}	1.222×10^{-11}	1.356×10^{-9}
12	4.458×10^{-14}	9.377×10^{-20}	4.992×10^{-16}	1.424×10^{-13}
13	1.117×10^{-5}	4.078×10^{-8}	5.151×10^{-6}	4.250×10^{-5}
14	6.481×10^{-8}	1.403×10^{-11}	8.575×10^{-9}	3.100×10^{-7}
15	6.506×10^{-11}	1.360×10^{-15}	8.479×10^{-12}	2.865×10^{-10}
16	1.089×10^{-14}	1.958×10^{-20}	1.190×10^{-16}	3.271×10^{-14}
17	1.102×10^{-5}	4.290×10^{-8}	4.959×10^{-6}	4.292×10^{-5}
18	1.849×10^{-8}	3.831×10^{-12}	2.364×10^{-9}	8.844×10^{-8}
19	5.273×10^{-12}	9.506×10^{-17}	1.828×10^{-13}	2.117×10^{-11}
20	7.591×10^{-16}	1.440×10^{-21}	7.601×10^{-18}	2.362×10^{-15}
Ok	3.748×10^{-5}	1.608×10^{-7}	1.721×10^{-5}	1.398×10^{-4}
Direct Exposure	1.971×10^{-6}	3.977×10^{-9}	5.705×10^{-7}	8.682×10^{-6}
Noble Gas	2.928×10^{-8}	1.248×10^{-11}	2.781×10^{-9}	1.350×10^{-7}
Radionuclide Release	4.864×10^{-12}	1.290×10^{-16}	1.229×10^{-13}	1.469×10^{-11}

Table 6. HTGR design parameters.

Parameter	Value	Unit
Thermal power	250	MWth
Number of fuel elements	420,000	-
Number of TRISO per fuel	12,000	-
Fuel type	$U0_2$ TRISO	-
Enrichment	8.9	%
Heavy metal per fuel elements	7	g
Average burn-up	90	GWd/tU
Fuel residence time	1057	Days
Diameter of pebble	60	mm
Fuel zone	50	mm

The end-of-life cycle core inventory activity and the release fractions are given in Table 7. ORIGEN 2.2 is a powerful and versatile tool used in the nuclear industry for the analysis and management of nuclear materials by calculating the nuclide composition and activity of fuel and other irradiated materials. It is used to predict the isotopic evolution of nuclear fuel, radioactive waste, and other materials over time, and to estimate the radioactive source term and decay heat of spent nuclear fuel and other irradiated materials. The ability to generate decay and fission product data for use in other computational codes enables the ORIGEN to be an essential tool for the design and analysis of advanced nuclear fuel cycles, as well as for the management and disposal of nuclear waste. It is available through the Standardized Computer Analysis for Licensing Evaluation package, which is maintained by the Oak Ridge National Laboratory [79–81].

Table 7. End-of-life cycle core inventory activity and the release fraction.

Chemical Group	Element or Isotope	Per Pebble Radioactivity (Ci)	10 Pebble Radioactivity (Ci)	100 Pebble Radioactivity (Ci)	Release Fraction
Noble Gas	Kr85	2.207×10^{-1}	2.207	2.207×10^{1}	1.00
	Kr87	1.939×10^{18}	1.939×10^{19}	1.939×10^{20}	1.00
	Kr88	1.266×10^{18}	1.266×10^{19}	1.266×10^{20}	1.00
	Xe133	4.797×10^{16}	4.797×10^{17}	4.797×10^{18}	1.00
	Xe135	1.335×10^{17}	1.335×10^{18}	1.335×10^{19}	1.00
Halogens	I131	1.553×10^{16}	1.553×10^{17}	1.553×10^{18}	1.00
	I132	7.164×10^{18}	7.164×10^{19}	7.164×10^{20}	2.00×10^{-2}
	I133	3.161×10^{17}	3.161×10^{18}	3.161×10^{19}	1.00
	I134	3.550×10^{19}	3.550×10^{20}	3.550×10^{21}	1.00
	I135	1.099×10^{18}	1.099×10^{19}	1.099×10^{20}	1.00
Alkali Metals	Cs134	1.517×10^{14}	1.517×10^{15}	1.517×10^{16}	1.00
	Cs136	2.650×10^{-1}	2.650	2.650×10^{1}	1.00
	Cs137	2.063	2.063×10^{1}	2.063×10^{2}	1.00
	Rb86	1.014×10^{-2}	1.014×10^{-1}	1.014	1.00
Chalcogens	Te127	3.541×10^{-1}	3.541	3.541×10^{1}	2.00×10^{-2}
	Te129	1.246	1.246×10^{1}	1.246×10^{2}	2.00×10^{-2}
	Te132	1.241×10^{17}	1.241×10^{18}	1.241×10^{19}	2.00×10^{-2}
Alkali Earths	Sr89	4.614	4.614×10^{1}	4.614×10^{2}	2.00×10^{-3}
	Sr90	1.821	1.821×10^{1}	1.821×10^{2}	2.00×10^{-3}
	Sr91	4.531×10^{17}	4.531×10^{18}	4.531×10^{19}	2.00×10^{-3}
	Ba140	8.507×10^{15}	8.507×10^{16}	8.507×10^{17}	2.00×10^{-3}
	Y90	2.010	2.010×10^{1}	2.010×10^{2}	2.00×10^{-3}
	Y91	6.083	6.083×10^{1}	6.083×10^{2}	1.00×10^{-1}
Transition Elements	Zr95	5.271×10^{15}	5.271×10^{16}	5.271×10^{17}	1.00×10^{-2}
	Zr97	2.666×10^{17}	2.666×10^{18}	2.666×10^{19}	1.00×10^{-2}
	Nb95	1.017×10^{16}	1.017×10^{17}	1.017×10^{18}	1.00×10^{-2}
Miscellaneous	Sb127	3.533×10^{-1}	3.533	3.533×10^{1}	1.00
	Sb129	1.260	1.260×10^{1}	1.260×10^{2}	1.00
	Mo99	1.004×10^{16}	1.004×10^{17}	1.004×10^{18}	1.00×10^{-6}
	Ru103	6.429×10^{15}	6.429×10^{16}	6.429×10^{17}	2.00×10^{-5}

Table 7. *Cont.*

Chemical Group	Element or Isotope	Per Pebble Radioactivity (Ci)	10 Pebble Radioactivity (Ci)	100 Pebble Radioactivity (Ci)	Release Fraction
	Ru105	1.093×10^{18}	1.093×10^{19}	1.093×10^{20}	2.00×10^{-5}
	Ru106	2.819	2.819×10^{1}	2.819×10^{2}	2.00×10^{-5}
Lanthanides	La140	4.263×10^{17}	4.263×10^{18}	4.263×10^{19}	1.00×10^{-6}
	Ce141	6.260×10^{15}	6.260×10^{16}	6.260×10^{17}	1.00×10^{-6}
	Ce143	2.527×10^{17}	2.527×10^{18}	2.527×10^{19}	1.00×10^{-6}
	Ce144	3.881×10^{14}	3.881×10^{15}	3.881×10^{16}	1.00×10^{-6}
	Pr143	7.236	7.236×10^{1}	7.236×10^{2}	1.00×10^{-6}
	Nd147	7.265×10^{15}	7.265×10^{16}	7.265×10^{17}	1.00×10^{-6}
	Np239	1.122×10^{18}	1.122×10^{19}	1.122×10^{20}	1.00×10^{-6}
Transuranic	Pu238	7.329×10^{1}	7.329×10^{2}	7.329×10^{3}	1.00×10^{-6}
	Pu239	6.029×10^{-2}	6.029×10^{-1}	6.029	1.00×10^{-6}
	Pu240	4.425	4.425×10^{1}	4.425×10^{2}	1.00×10^{-6}
	Pu241	2.105×10^{-1}	2.105	2.105×10^{1}	1.00×10^{-6}
	Am241	6.758×10^{-1}	6.758	6.758×10^{1}	1.00×10^{-6}

4.6. Radiological Consequence Analysis by Using MicroShield

With the tabulated source data from the MST analysis and shielding material information, the radiological consequence can be quantified through the MicroShield. The MicroShield is used to model the source and shielding by determining their geometrical shapes and compositions of them. Additionally, the dose points can be selected to identify the consequences at the specific points. In this paper, the absorbed dose rate and exposure rate at 5 km from the source for three predetermined release categories (RR, NG, and DE) are calculated. Based on multiple independent variables, a sensitivity study is implemented to identify the impact of the input variables in this section.

4.6.1. Case Study 1

The first case study is to calculate the exposure rate and absorbed dose rate of each release category for quantification of the consequences. To simulate the radionuclide transport from the source, the shielding arrangement should be determined. As we can see in Figure 9, the cylinder volume geometry is selected for assuming a radioactive source at the bottom of a pebble fuel-filled canister. As mentioned above, there are two concrete walls as safety barriers: the inside wall between the canister and storage building and the outside wall between the inside wall and the environment. In the case of DE, the safety barriers function as the shielding, however, in the case of RR and NG, the radioactive materials bypass the concrete walls because of the HVAC system's operation status. Table 8 demonstrates the dimensions and material information for the shielding. Table 9 shows the exposure rate and absorbed dose rate as the consequence of each release category when only one pebble has failed at the center of the canister. As mentioned above, it is assumed that the radioactivity is detected at 5 km from the source on the X-axis.

4.6.2. Case Study 2—Sensitivity Study

The second case study is a sensitivity study to analyze the impact of the input variables. As shown in Table 10, 189 case datasets are generated to identify the input variables: the number of failed pebbles, the location of the failed pebbles, the inside wall thickness, and the outside wall thickness. The location of the failed pebble is equivalent to the distance between the canister and the source that depends on the number of failed pebbles because

a number of pebbles occupy a large volume in the canister. Therefore, as the number of failed pebbles increases, the shorter the distance between the canister and source in the MicroShield model. The distance is varied from the source to zero which indicates that the location of the failed pebble moves from the center to the canister's surface.
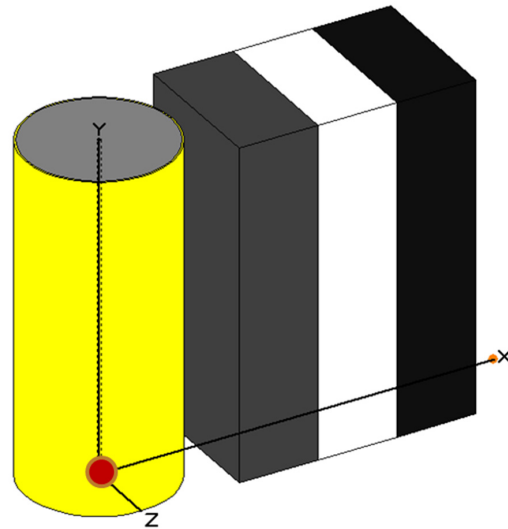
Figure 9. Radiological Consequence Simulation for Spent Pebble Fuel Failure in a Canister in MicroShield.

Table 8. Dimensions and Material Information for the Shielding.

	Material	Height (cm)	Thickness (cm)
Pebbles in the canister	Graphite		89
Canister	304 SL		2.5
Air-gap between the canister and the inside wall	Air		30
Inside wall (silo well)	Barite concrete	418	100
Air-gap between the inside wall and outside wall	Air		100
Outside wall (SFSS building)	NBS concrete		100

Table 9. Exposure Rate and Absorbed Dose Rate for Each Release Category.

Release Categories	Exposure Rate (mR/h)	Absorbed Dose Rate (mrad/h)
Radionuclide Release	1.63×10^{-6}	1.42×10^{-6}
Noble Gas	1.41×10^{-8}	1.23×10^{-8}
Direct Exposure	7.39×10^{-10}	6.45×10^{-10}

Table 10. Dataset Generation from the Input Variables.

Input Variables	Range	Numbers
Number of failed pebbles	1 to 30,000	7
Distance between canister surface and source	From the source to 0	3
Inside wall thickness	[75, 100, 125]	3
Outside wall thickness	[75, 100, 125]	3
Total number of datasets	189	

For the sensitivity analysis method, ordinary least square (OLS) is used to estimate the linearity of the parameters that implies the relationship between independent variables and one dependent variable. The linear regression analysis fitting the coefficients is to directly measure the impact from the sensitivity perspective [82]. The OLS parameter is updated to minimize the sum of the squared residual which is a discrepancy between the observed values and the corresponding fitted values. The equation of the OLS is as follows:

$$y_i = x_i^T \beta + \varepsilon_i$$

where x_i (k by 1 vector) and y_i are regressor (or predictor) and response in i-th observation, respectively. β (k by 1 vector) is a vector of unknown parameters and ε_i is a random variable that refers to the vertical distance between the actual values and fitted values. The residual $(S(b))$ can be calculated by the following equation where b is a candidate value for the β:

$$S(b) = \sum_{i=1}^{n} \left(y_i - x_i^T b \right)^2 = (y - Xb)^T (y - Xb)$$

The parameter $\hat{\beta}$ can be found by minimizing the residual in the equation below:

$$\hat{\beta} = arg\min_{b \in \mathrm{R}} S(b) = \left(\frac{1}{n} \sum_{i=1}^{n} x_i x_i^T \right)^{-1} \frac{1}{n} \sum_{i=1}^{n} x_i y_i = \left(X^T X \right)^{-1} X^T y$$

where X is the n by k design matrix. After beta estimation, the predicted value ($\hat{y}$) would be calculated:

$$\hat{y} = X\hat{\beta}$$

To assess the goodness-of-fit of the regression model, R-squared is used by measuring a ratio of 'predicted' variance to the 'actual' of the dependent variable. It represents how closely the observed data points are to the explained regression line. The R-squared is given by:

$$R^2 = \frac{\sum \left(\hat{y}_i - \bar{y} \right)^2}{\sum \left(y_i - \bar{y} \right)^2}$$

The sensitivity analysis results are summarized in Table 11 below. There are two cases for the sensitivity study: (A) exposure rate at the outside of the storage (10 m from the source) and (B) EAB. Before implementing the OLS method, data points are standardized because the input variables have different units and material characteristics. The results are summarized as:

- R-squared is low in the case of A, whereas, case B has a very high R-squared value (=1).
- The *p*-values are very low in both cases (*p*-value < 0.05).
- For case A, both the R-squared and the *p*-value are low. It indicates that the regression model discloses a significant statistical effect of input variables on response but is not good at predicting the responses from the input variables accurately because of unexplained variance. In other words, the data points are distributed further from the regression line. Whereas, the regression model for case B not only explains the responses well but also is able to predict the output accurately.

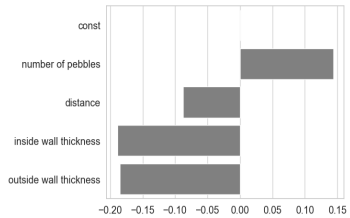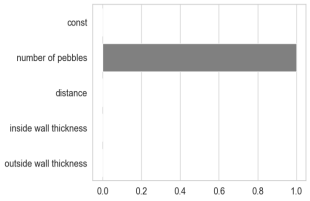**Table 11.** Ordinary Least Square Method Results.

Exposure Rate	At the Outside of the Storage (A)	At the EAB (B)
Distance from the source	10 m	5 km
R-squared	0.108	1.00
p-value for goodness-of-fit test	2.89×10^{-4}	0

4.6.3. Discussion for Sensitivity Study

The major findings from the sensitivity study results shown in Table 12 are as follows.

Table 12. Sensitivity Analysis Results for Exposure Rate at the Outside of the Storage and EAB.

Impact Variables	At the Outside of the Storage (A)	At the EAB (B)
Number of pebbles	1.438×10^{-1}	1
Distance	-8.78×10^{-2}	-3.557×10^{-5}
Inside wall thickness	-1.889×10^{-1}	1.388×10^{-17}
Outside wall thickness	-1.848×10^{-1}	-1.735×10^{-17}
Sensitivity for case A		Sensitivity for case B

- Findings for case A are:
  - The order of the impact of the input variables is as follows: the inside wall thickness, the outside wall thickness, the number of pebbles, and the distance between the source and the canister surface. However, the difference between the coefficients of the inside wall thickness and the outside wall thickness is small.
  - Therefore, the wall thickness is the most significant variable to determine the exposure rate at the outside of the storage regardless of whether it is the inside wall or the outside wall.
  - Only the number of failed pebbles is positively sensitive to the exposure rate which means more failed pebble numbers and a larger exposure rate. Otherwise, the exposure rate decreases when the variables increase.
- Findings for case B are:
  - The coefficient of the number of pebbles is very high (=1) and the others' coefficients are extremely low. In other words, the number of pebbles is a dominant input variable for case B. The exposure rate at 5 km from the source does not depend on the distance and wall thickness because they are negligible compared to the EAB.

The OLS regression model can be misinterpreted in the impact analysis when there is collinearity between input variables. Thus, it is required to confirm the characteristics of independent variables in the input variable selection process. Moreover, since the OLS model is limited to predicting a single response variable, multi-output regression by using deep learning is recommended when there are two or more output variables.

4.7. Risk Integration for F-C Curve

The measure of risk considering frequency and consequence for an initiating event is given by the following equation [5]:

$$R = f \sum_{n=1}^{m} P_n K_n$$

where R is a risk, f is the frequency of the initiating event, which is a canister drop, and P_n and K_n are conditional probability in a given initiating event and corresponding

consequence of n-th event sequence, respectively. Table 13 shows the integrated risk for each release category for one pebble failure case.

Table 13. Risk Integration for Each Release Category.

Release Categories	Consequence (mrad/h)	Consequence (30 Days-REM)	Frequency (/Year)	Risk (REM/Year)
Radionuclide Release	1.42×10^{-6}	1.022×10^{-6}	4.352×10^{-12}	4.449×10^{-18}
Noble Gas	1.23×10^{-8}	8.856×10^{-9}	2.901×10^{-8}	2.569×10^{-16}
Direct Exposure	7.39×10^{-10}	5.321×10^{-10}	2.021×10^{-6}	1.075×10^{-15}

In addition to the integrated risk assessment for the non-LWR PRA approach, Frequency-Consequence (F-C) target is used to evaluate the risk significance by comparing it against evaluation criteria derived from regulatory requirements and NEI 18-04 methodology [27]. The NEI 18-04 F-C target line, a black line shown in Figure 10, is also used to identify the risk margins that could be evidence of defense-in-depth methodology application. The figure below illustrates criterion lines for the F-C target, risk-significant LBE (black dash line under the F-C target line), and LBEs, such as anticipated operational occurrences (AOOs), Design Basis Events (DBEs), and Beyond DBE (BDBEs)—black dash vertical and horizontal grid lines. In this research, release categories' frequency with uncertainties (5th percentile, median, mean, and 95th percentile) and consequences are compared with the target line in the F-C curve when the failed pebbles are 1, 100, and 10,000. Overall, the frequencies and doses, including their uncertainty, for all the scenarios analyzed, meet the NEI 18-04 F-C target and the risk-significant LBE criterion.
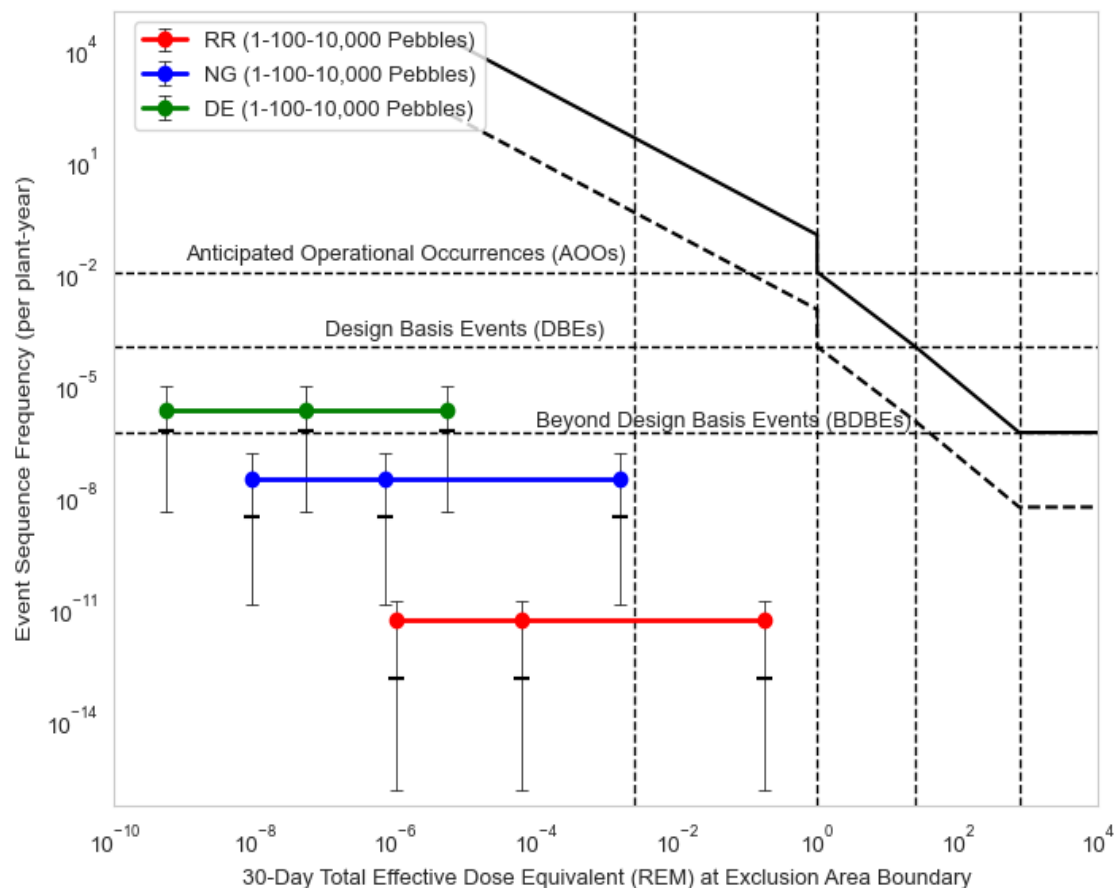
Figure 10. F-C Curve for Spent Pebble fuel-filled Dry Cask PRA.

5. Conclusions

In this research, the spent pebble fuel-filled dry cask PRA is performed in accordance with the PRA standard for the advanced non-LWR power plant. While TRISO-coated pebble fuel is in the spotlight as the fuel for the advanced reactor type, there is a lack of comprehensive study on the dry cask PRA for spent pebble fuel. Thus, this research investigates how the various PRA elements are systematically connected from the IE identification to the risk integration and applied to the pebble-filled dry cask PRA by demonstrating a case study. The ultimate goal of the research is to illustrate how the PRA elements are logically and structurally implemented by using existing methodologies, available data, and tools to contribute to risk-informing the design and operation of a dry cask storage system for spent pebble fuel.

To summarize the workflow in this paper, the MLD identified a canister vertical drop event as the selected IE from the varied height in an SFSS silo. From the given IE, the event tree is established through the pivot events determined by the pebble failure, canister damage, and HVAC system operation system states. The Phoenix Architecture tools are used to quantify the sequence and corresponding uncertainties of the release categories, such as direct exposure, noble gas, and radionuclide release. ORIGEN and MicroShield are used to quantify the radiological consequences of the dropped canister. The OLS methodology is utilized to identify the impact of each independent variable, including the number of failed pebbles, their location, and wall thickness, for exposure rate at the outside of the building and the EAB from the sensitivity study perspective. Finally, the risk is quantified and compared with the NEI 18-04 F-C target to confirm how much the risk would be for the given event scenarios at the EAB. Overall, the frequencies and doses, including their uncertainty, for all the scenarios analyzed, meet the NEI 18-04 F-C target and the risk-significant LBE criterion.

The challenge of this study Is the uncertainty stemming from the data and simulation model due to the lack of information and knowledge. From the uncertainty perspective in this paper, there are two types of uncertainties: epistemic and aleatory uncertainty. Although the CNID method is employed to reduce epistemic uncertainty by quantifying the event sequence frequency, additional studies are needed to determine the failure probabilities of the pebble and canister. Moreover, as the validation study for the number of damaged pebbles resulting from canister drop was implemented by comparing computational simulation and experimental results, it is recommended to conduct further validation studies to reduce uncertainties.

As mentioned earlier, the purpose of this paper is to explicitly demonstrate the PRA workflow through a case study. To simplify the process of examining the PRA elements, the scope of the PRA standard is delimited by selecting one IE and establishing assumptions, such as limiting the canister-dropping scenario and assuming state of sources in the canister. Thus, the PRA workflow can be extended to apply to the full scope of the PRA technical requirements, including the full scope of the iEs, by using not only the MLD but also FMEA or HBFT. Moreover, the CCF parameter estimation utilized the PRA model which could be considered as the extended scope of the PRA elements for SFSS design and operation. By developing a multi-variable and multi-output regression model based on the machine learning algorithm, the sensitivity study would be advanced not only to analyze the impact of the variable but also to evaluate the safety functions or barriers.

Author Contributions: Conceptualization, M.A.D.; Methodology, H.T., M.M.H., Y.A.A. and M.A.D.; Formal analysis, H.T., M.M.H. and Y.A.A.; Investigation, H.T. and M.A.D.; Data curation, J.L.; Writing—original draft, J.L., H.T. and M.A.D.; Writing—review & editing, M.M.H. and Y.A.A.; Visualization, J.L. and H.T.; Supervision, M.A.D.; Funding acquisition, M.A.D. All authors have read and agreed to the published version of the manuscript.

Data Availability Statement: Data available on request.

Conflicts of Interest: The authors declare no conflict of interest.

Abbreviation

ANL	Argonne National Laboratory
AOO	Anticipated Operational Occurrence
BDBA	Beyond Design Basis Accident
CCF	Common Cause Failure
CDF	Core Damage Frequency
CNID	Constrained Noninformative Distribution
DA	Data Analysis
DBA	Design Basis Accident
DE	Direct Exposure
EAB	Exclusion Area Boundary
ESA	Event Sequence Analysis
ESQ	Event Sequence Quantification
ET	Event Tree
F-C	Frequency-Consequence
FEM	Finite Element Model
FHS	Fuel Handling System
FMEA	Failure Modes and Effort Analysis
FP	Fission Product
HAZOP	Hazard and Operability Analysis
HBFT	Heat Balance Fault Tree
HTR-PM	High-Temperature Gas-Cooled Reactor-Pebble Bed Module
HVAC	Heating, Ventilation, and Air Conditioning
IE	Initiating Event
INL	Idaho National Laboratory
IPyC	Inner Pyro-Carbon
LAR	License Amendment Requests
LBE	Licensing Basis Event
LERF	Large Early Release Frequency
LMP	Licensing Modernization Project
LWR	Light Water Reactor
MLD	Master Logic Diagram
MST	Mechanistic Source Term
NG	Noble Gas
NPP	Nuclear Power Plant
NRC	Nuclear Regulatory Commission
OLS	Ordinary Least Square
OPyC	Pyro-Carbon
ORNL	Oak Ridge National Laboratory
PBR	Pebble Bed Reactors
PHA	Process Hazards Analysis
PRA	Probabilistic Risk Assessment
RCA	Radiological Consequence Analysis
RI	Risk Integration
RR	Radionuclide Release
SFCLS	Spent Fuel Conveying and Loading System
SiC	Silicon Carbide

SNF	Spent Nuclear Fuel
SSC	Structures, Systems, and Components
TRISO	Tri-Structural Isotropic
VHTR	Very High-Temperature Gas Reactor

References

1. Bunn, M.; Holdren, J.P.; Macfarlane, A.; Pickett, S.E.; Suzuki, A.; Suzuki, T.; Weeks, J. *Project on Managing the Atom*; Belfer Center for Science and International Affairs: Cambridge, MA, USA, 2012; p. 146.
2. Romanato, L.S. Advantages of dry hardened cask storage over wet storage for spent nuclear fuel. In Proceedings of the 2011 International Nuclear Atlantic Conference—INAC 2011, Belo Horizonte, Brazil, 24–28 October 2011; p. 9.
3. Werner, J.D. *U.S. Spent Nuclear Fuel Storage*; R42513; Congressional Research Service Report for Congress: Washington, DC, USA, 2012; p. 57.
4. Sekiguchi, Y. *Mitigating the Risks of Spent Nuclear Fuel in Japan*; Center for Strategic and International Studies: Washington, DC, USA, 2017; p. 9.
5. Malliakos, A. *A Pilot Probabilistic Risk Assessment of a Dry Cask Storage System at a Nuclear Power Plant (NUREG-1864)*; US NRC: Washington, DC, USA, 2007.
6. JBiersdorf, M.; Eidelpes, E.F. *Development of Dry Cask Risk Tools*; INL/EXT-20-57570-Rev000, 1603757; U.S. Department of Energy: Oak Ridge, TN, USA, 2020. [CrossRef]
7. Fort, J.; Richmond, D.; Cuta, J.; Suffield, S. *Thermal Modeling of the TN-32B Cask for the High Burnup Spent Fuel Data Project*; PNNL-28915, 1566774; U.S. Department of Energy: Oak Ridge, TN, USA, 2019. [CrossRef]
8. Koskenranta, J.; Paavola, I.; Hotakainen, R.; Laato, T. Loviisa Nuclear Power Plant Spent Fuel Storage Risk Analysis. In Proceedings of the Probabilistic Safety Assessment and Management, PSAM 16, Honolulu, HI, USA, 26 June–1 July 2022; p. 12.
9. Olofsson, F.; Olsson, A. Challenges and Lessons Learned from a PSA on a Spent Fuel Pool Facility. In Proceedings of the Probabilistic Safety Assessment and Management, PSAM16, Honolulu, HI, USA, 26 June–1 July 2022; p. 7.
10. Kadak, A.C. A future for nuclear energy: Pebble bed reactors. *IJCIS* **2005**, *1*, 330. [CrossRef]
11. Brey, H.L. *Current Status and Future Development of Modular High Temperature Gas Cooled Reactor Technology*; IAEA-TECDOC-1198; IAEA, Nuclear Power Technology Development Section: Vienna, Austria, 2001.
12. INL. *Modular HTGR Safety Basis and Approach*; INL/EXT-11-22708; Idaho National Laboratory (INL): Idaho Falls, ID, USA, 2011.
13. Del Cul, G.D. *TRISO-Coated Fuel Processing to Support High Temperature Gas-Cooled Reactors*; ORNL/TM-2002/156, 814326; ORNL: Oak Ridge, TN, USA, 2002. [CrossRef]
14. Gen IV International Forum. *GIF Annual Report 2021*; Gen IV International Forum: Brussels, Belgium, 2021.
15. Moses, D.L. *Very High-Temperature Reactor (VHTR) Proliferation Resistance and Physical Protection (PR&PP)*; ORNL/TM-2010/163, 1027406; ORNL: Oak Ridge, TN, USA, 2011. [CrossRef]
16. Kovacic, D.; Gibbs, P.; Worrall, L.; Hunneke, R.; Harp, J.; Hu, J. *Advanced Reactor Safeguards: Nuclear Material Control and Accounting for Pebble Bed Reactors*; Oak Ridge National Laboratory: Oak Ridge, TN, USA, 2021.
17. Kovacic, D.; Gibbs, P.; Scott, L. *Model MC&A Plan for Pebble Bed Reactors*; Oak Ridge National Laboratory: Oak Ridge, TN, USA, 2020.
18. Hu, R.; Hu, G.; Zou, L.; Klingberg, A.; Fei, T.; Nunez, D. *FY20 SAM Code Developments and Validations for Transient Safety Analysis of Advanced Non-LWRs*; ANL/NSE-20/50, 1716517, 162791; U.S. Department of Energy: Oak Ridge, TN, USA, 2020. [CrossRef]
19. Novak, A.J.; Carlsen, R.W.; Schunert, S.; Balestra, P.; Reger, D.; Slaybaugh, R.N.; Martineau, R.C. Pronghorn: A Multidimensional Coarse-Mesh Application for Advanced Reactor Thermal Hydraulics. *Nucl. Technol.* **2021**, *207*, 1015–1046. [CrossRef]
20. Laboure, V.; Ortensi, J.; Hermosillo, A.; Strydom, G.; Balestra, P. *FY21 Status Report on the ART-GCR CMVB and CNWG International Collaborations, ART-M3AT-21IN0603011*; Idaho National Laboratory (INL): Idaho Falls, ID, USA, 2021.
21. IAEA. *Evaluation of High Temperature Gas Cooled Reactor Performance: Benchmark Analysis Related to the PBMR-400, PBMM, GT-MHR, HTR-10 and the ASTRA Critical Facility*; International Atomic Energy Agency: Vienna, Austria, 2013.
22. Zhang, Z.-Y.; Dong, Y.-J.; Shi, Q.; Li, F.; Wang, H.-T. 600-MWe high-temperature gas-cooled reactor nuclear power plant HTR-PM600. *Nucl. Sci. Tech.* **2022**, *33*, 101. [CrossRef]
23. Joksimovic, V.; Houghton, W.J.; Emon, D.E. HTGR Risk Assessment Study. In Proceedings of the International Conference on Nuclear Systems Reliability Engineering and Risk Assessment, Gatlinburg, TN, USA, 20 June 1977; General Atomics: San Diego, CA, USA, 1977. Available online: https://www.osti.gov/biblio/5450842-htgr-risk-assessment-study (accessed on 26 September 2021).
24. Herczeg, J. *Probabilistic Risk Assessment for The Standard Modular High Temperature Gas-Cooled Reactor, DOE-HTGR-86-011*; Civilian Reactor Development, Office of Nuclear Energy: Washington, DC, USA, 1987.
25. Savkina, M.D. *Probabilistic Accident Analysis of the Pebble Bed Modular Reactor for Use with Risk Informed Regulation*; MIT: Cambridge, MA, USA, 2004; Available online: https://dspace.mit.edu/bitstream/handle/1721.1/17748/56504086-MIT.pdf?sequence=2&isAllowed=y (accessed on 29 September 2021).
26. Demkowicz, P.A.; Liu, B.; Hunn, J.D. Coated particle fuel: Historical perspectives and current progress. *J. Nucl. Mater.* **2019**, *515*, 434–450. [CrossRef]

27. Moe, W.L.; Afzali, A. *Modernization of Technical Requirements for Licensing of Advanced Non-Light Water Reactors Selection and Evaluation of Licensing Basis Events*; INL/EXT-19-55513-Rev1; Idaho National Lab. (INL): Idaho Falls, ID, USA, 2020. [CrossRef]

28. Moe, W.L.; Afzali, A. *Modernization of Technical Requirements for Licensing of Advanced Non-Light Water Reactors: Safety Classification and Performance Criteria for Structures, Systems, and Components*; INL/EXT-19-55516-Rev000; SC-29980-102.Rev0; Idaho National Lab. (INL): Idaho Falls, ID, USA; Southern Company Services: Birmingham, AL, USA, 2019. [CrossRef]

29. Fleming, K.; Wallace, E.; Afzali, A. Use of PRA to Select Licensing Basis Events. In *PSAM14*; UCLA: Los Angeles, CA, USA, 2018; p. 12.

30. US NRC. *NRC Non-Light Water Reactor (Non-LWR) Vision and Strategy, Volume 3—Computer Code Development Plans for Severe Accident Progression, Source Term, and Consequence Analysis*; US NRC: Washington, DC, USA, 2020.

31. ASME. *Probabilistic Risk Assessment Standard for Advanced Non-LWR Nuclear Power Plants*; ANS, ASME/ANS RA-S-1.4-2021; ASME: New York, NY, USA, 2021.

32. Braverman, J.I.; Morante, R.J.; Xu, J.; Hofmayer, C.H.; Shaukat, S.K. *Impact Analysis of Spent Fuel Dry Casks under Accidental Drop Scenarios*; U.S. Department of Energy: Oak Ridge, TN, USA, 2003; Volume BNL-NUREG-71196-2003-CP, p. 8.

33. Lin, M.; Li, Y. Analysis of the interactions between spent fuel pebble bed and storage canister under impact loading. *Nucl. Eng. Des.* **2020**, *361*, 110548. [CrossRef]

34. Lin, M.; Wang, J.; Wu, B.; Li, Y. Dynamic analysis of dry storage canister and the spent fuels inside under vertical drop in HTR-PM. *Ann. Nucl. Energy* **2021**, *154*, 108030. [CrossRef]

35. IAEA. *Defining Initiating Events for Purposes of Probabilistic Safety Assessment*; IAEA-TECDOC-719; IAEA: Vienna, Austria, 1993.

36. Garrick, B.J.; Fleming, K.N. *Seabrook Station Probabilistic Safety Assessment*; PLG-0242; Pickard, Lowe and Garrick, Inc.: Newport Beach, CA, USA, 1982.

37. Papazoglou, I.A.; Aneziris, O.N. Master Logic Diagram: Method for hazard and initiating event identification in process plants. *J. Hazard. Mater.* **2003**, *97*, 11–30. [CrossRef]

38. Cho, N.-C.; Jae, M.; Joon-Eon, Y. Initiating Events Identification of the IS Process Using the Master Logic Diagram. In Proceedings of the Korean Nuclear Society Conference, Taejon, Republic of Korea, 11–13 April 2005; pp. 55–56.

39. Purba, J.H. Master Logic Diagram: An Approach to Identify Initiating Events of HTGRs. *J. Phys. Conf. Ser.* **2018**, *962*, 012036. [CrossRef]

40. Lee, H.; Park, J. Analysis of Initiating Events for SMART using Heat Balance Fault Tree Method. In Proceedings of the Korean Nuclear Society, Jeju, Republic of Korea, 14–20 April 2017; p. 4.

41. Han, S.; Park, J.; Jang, S. *Identification of Initiating Events Using the Master Logic Diagram in Low-Power and Shutdown PSA for Nuclear Power Plant*; KAERI/TR-2497/2003; KAERI: Daejeon, Republic of Korea, 2003.

42. Liu, H.-C.; Liu, L.; Liu, N. Risk evaluation approaches in failure mode and effects analysis: A literature review. *Expert Syst. Appl.* **2013**, *40*, 828–838. [CrossRef]

43. Aldemir, T.; Stovsky, M.P.; Kirschenbaum, J.; Mandelli, D.; Bucci, P.; Mangan, L.A.; Miller, D.W.; Sun, X.; Ekici, E.; Guarro, S.; et al. *Dynamic Reliability Modeling of Digital Instrumentation and Control Systems for Nuclear Reactor Probabilistic Risk Assessments*; NUREG/CR-6942; Ohio State University: Columbus, OH, USA, 2007.

44. Gaol, F.L.; Nguyen, Q.V. (Eds.) *Proceedings of the 2011 2nd International Congress on Computer Applications and Computational Science*; Springer: Berlin/Heidelberg, Germany, 2012; Volume 144. [CrossRef]

45. Cadwallader, L.C. *Preliminary Failure Modes and Effects Analysis of the US DCLL Test Blanket Module*; U.S. Department of Energy: Oak Ridge, TN, USA, 2010; p. 158.

46. Bright, M.; Foster, R.; Hampton, C.; Ruiz, J.; Moeller, B. Failure modes and effects analysis for surface-guided DIBH breast radiotherapy. *J. Appl. Clin. Med. Phys.* **2022**, *23*, e13541. [CrossRef] [PubMed]

47. Huq, M.S.; Fraass, B.A.; Dunscombe, P.B.; Gibbons, J.P., Jr.; Ibbott, G.S.; Mundt, A.J.; Mutic, S.; Palta, J.R.; Rath, F.; Thomadsen, B.R.; et al. The report of Task Group 100 of the AAPM: Application of risk analysis methods to radiation therapy quality management: TG 100 report. *Med. Phys.* **2016**, *43*, 4209–4262. [CrossRef] [PubMed]

48. Li, S.; Zeng, W. Risk analysis for the supplier selection problem using failure modes and effects analysis (FMEA). *J. Intell. Manuf.* **2016**, *27*, 1309–1321. [CrossRef]

49. Chi, C.-F.; Sigmund, D.; Astardi, M.O. Classification Scheme for Root Cause and Failure Modes and Effects Analysis (FMEA) of Passenger Vehicle Recalls. *Reliab. Eng. Syst. Saf.* **2020**, *200*, 106929. [CrossRef]

50. Sowder, A. *Program on Technology Innovation: Early Integration of Safety Assessment into Advanced Reactor Design—Preliminary Body of Knowledge and Methodology*; 2018 Technical Report 3002011801; Electric Power Research Institute: Palo Alto, CA, USA, 2018.

51. Marciulescu, C. *Program on Technology Innovation: Early Integration of Safety Assessment into Advanced Reactor Design—Project Capstone Report*; 2019 Technical Report 3002015752; Electric Power Research Institute: Palo Alto, CA, USA, 2019.

52. Rimkevičius, S.; Vaišnoras, M.; Babilas, E.; Ušpuras, E. HAZOP application for the nuclear power plants decommissioning projects. *Ann. Nucl. Energy* **2016**, *94*, 461–471. [CrossRef]

53. Joubert, J.; Kohtz, N.; Coe, I. South African Safety Assessment Framework for the Pebble Bed Modular Reactor. In *Fourth International Topical Meeting on High Temperature Reactor Technology, Volume 2*; ASME: Washington, DC, USA, 2008; pp. 193–203. [CrossRef]

54. Afzali, A. *Molten Salt Reactor Experiment (MSRE) Case Study Using Risk-Informed, Performance—Based Technical Guidance to Inform Future Licensing for Advanced Non-Light Water Reactors*; EPRI AR LR 2019-06; Southern Company: Atlanta, GA, USA, 2019.

55. Taylor, J.M. *Issues Pertaining to the Advanced Reactor (Prism, Mhtgr, And Pius) And Candu 3 Designs and Their Relationship to Current Regulatory Requirements*; SECY-93-092; US NRC: Washington, DC, USA, 1993.

56. Andrews, N.; Nenoff, T.; Luxat, D.; Clark, A.; Leute, J. *Mechanistic Source Term Considerations for Advanced Non-LWRs*; SAND--2020-6730, 1638572, 687170; U.S. Department of Energy: Oak Ridge, TN, USA, 2020. [CrossRef]

57. Moe, W.L. *Risk-Informed Performance-Based Technology Inclusive Guidance for Advanced Reactor Licensing Basis Development*; INL/EXT-19-55375-Rev000; Idaho National Lab. (INL): Idaho Falls, ID, USA, 2019. [CrossRef]

58. US NRC. *White Paper on Options for Risk Metrics for New Reactors*; US NRC: Washington, DC, USA, 2009.

59. Boyer, R.L. *Probabilistic Risk Assessment (PRA): Analytical Process for Recognizing Design and Operational Risks*; Safety & Mission Assurance (S&MA), NASA Johnson Space Center: Houston, TX, USA, 2017.

60. Phillips, J.A.; Nagley, S.G.; Shaber, E.L. Fabrication of uranium oxycarbide kernels and compacts for HTR fuel. *Nucl. Eng. Des.* **2012**, *251*, 261–281. [CrossRef]

61. Seibert, R.L.; Jolly, B.C.; Balooch, M.; Schappel, D.P.; Terrani, K.A. Production and characterization of TRISO fuel particles with multilayered SiC. *J. Nucl. Mater.* **2019**, *515*, 215–226. [CrossRef]

62. Bruna, G.B.; Bourgois, T.; Ivanov, E.; Monhardt, D. *Overview of Generation IV (Gen IV) Reactor Designs*; IRSN Report 2012/158; IRSN: Paris, France, 2012.

63. Morris, R.N.; Petti, D.A.; Powers, D.A.; Boyack, B.E. *TRISO-Coated Particle Fuel Phenomenon Identification and Ranking Tables (PIRTs) for Fission Product Transport Due to Manufacturing, Operations and Accidents*; NUREG/CR-6844; US NRC: Washington, DC, USA, 2004; Volume 1.

64. Kwapis, E.H.; Liu, H.; Hartig, K.C. Tracking of individual TRISO-fueled pebbles through the application of X-ray imaging with deep metric learning. *Prog. Nucl. Energy* **2021**, *140*, 103913. [CrossRef]

65. Moormann, R.; Kemp, R.S.; Li, J. Caution Is Needed in Operating and Managing the Waste of New Pebble-Bed Nuclear Reactors. *Joule* **2018**, *2*, 1911–1914. [CrossRef]

66. Wu, B.; Wang, J.; Li, Y.; Wang, H.; Ma, T. Design, Experiment, and Commissioning of the Spent Fuel Conveying and Loading System of HTR-PM. *Sci. Technol. Nucl. Install.* **2022**, *2022*, e1817191. [CrossRef]

67. Wang, J.; Zhang, Z.; Wu, B.; Li, Y. Design of the HTR-PM Spent Fuel Storage Facility. In Proceedings of the 7th International Topical Meeting on High Temperature Reactor Technology: The Modular HTR Is Advancing towards Reality Papers and Presentations, Weihai, China, 27–31 October 2014; p. v.

68. Wang, J.; Wang, B.; Wu, B.; Li, Y. Design of the Spent Fuel Storage Well of HTR-PM. In Proceedings of the 2016 24th International Conference on Nuclear Engineering, Charlotte, NC, USA, 26–30 June 2016. [CrossRef]

69. Ma, Z.; Kvarfordt, K.; Wierman, T. *Industry-Average Performance for Components and Initiating Events at U.S. Commercial Nuclear Power Plants: 2020 Update*; INL/EXT-21-65055-Rev000, 1847110; Idaho National Lab. (INL): Idaho Falls, ID, USA, 2022. [CrossRef]

70. Atwood, C.L.; LaChance, J.; Martz, H.F.; Anderson, D.J.; Englehardt, M.; Whitehead, D.; Wheeler, T. *Handbook of Parameter Estimation for Probabilistic Risk Assessment*; NUREG/CR-6823; Sandia National Lab.: Albuquerque, NM, USA, 2003.

71. IAEA. Performance of Engineered Barrier Materials in Near Surface Disposal Facilities for Radioactive Waste. International Atomic Energy Agency, Text. 2001. Available online: https://www.iaea.org/publications/6297/performance-of-engineered-barrier-materials-in-near-surface-disposal-facilities-for-radioactive-waste (accessed on 10 March 2023).

72. Severe Accident Risks: An Assessment for Five U.S. Nuclear Power Plants—Final Summary Report (NUR. NRC Web). Available online: https://www.nrc.gov/reading-rm/doc-collections/nuregs/staff/sr1150/v1/index.html (accessed on 6 January 2023).

73. IAEA. Handbook of Parameter Values for the Prediction of Radionuclide Transfer in Terrestrial and Freshwater Environments. International Atomic Energy Agency, Text. 2010. Available online: https://www.iaea.org/publications/8201/handbook-of-parameter-values-for-the-prediction-of-radionuclide-transfer-in-terrestrial-and-freshwater-environments (accessed on 10 March 2023).

74. Sailor, V.L.; Perkins, K.R.; Weeks, J.R.; Connell, H.R. *Severe Accidents in Spent Fuel Pools in Support of Generic Safety, Issue 82*; Div. of Reactor and Plant Systems, NUREG/CR-4982; BNL-NUREG-52093; Brookhaven National Lab. (BNL): Upton, NY, USA; Nuclear Regulatory Commission: Washington, DC, USA, 1987. [CrossRef]

75. Travis, R.J.; Davis, R.E.; Grove, E.J.; Azarm, M.A. *A Safety and Regulatory Assessment of Generic BWR and PWR Permanently Shutdown Nuclear Power Plants*; Div. of Regulatory Applications; NUREG/CR-6451; BNL-NUREG-52498; US Nuclear Regulatory Commission (NRC): Washington, DC, USA; Brookhaven National Lab. (BNL): Upton, NY, USA, 1997. [CrossRef]

76. U.S. Nuclear Regulatory Commission. *Population-Related Siting Considerations for Advanced Reactors*; NRC Staff Prepared White Paper; U.S. Nuclear Regulatory Commission: Rockville, MD, USA, 2019.

77. Moore, R.L.; Oh, C.H.; Merrill, B.J.; Petti, D.A. *Studies on Air Ingress for Pebble Bed Reactors*; IAEA: Vienna, Austria, 2002.

78. Hadad, Y.; Jafarpur, K. Modeling of Laminar Forced Convection Heat Transfer in Packed Beds with Pebbles of Arbitrary Geometry. *J. Por. Media* **2013**, *16*, 1049–1061. [CrossRef]

79. Zheng, M.; Tian, W.; Wei, H.; Zhang, D.; Wu, Y.; Qiu, S.; Su, G. Development of a MCNP–ORIGEN burn-up calculation code system and its accuracy assessment. *Ann. Nucl. Energy* **2014**, *63*, 491–498. [CrossRef]

80. Bowman, S.M. SCALE 6: Comprehensive Nuclear Safety Analysis Code System. *Nucl. Technol.* **2011**, *174*, 126–148. [CrossRef]

81. Ismail, A.S.; Takip, K.M.; Mustafa, M.K.A.; Anwar, A. RTP: Radionuclides Inventories Calculation Using Origen Code. In Proceedings of the R and D Seminar 2012: Research and Development Seminar 2012, Bangi, Malaysia, 26–28 September 2012.

82. Mohantyl, S. Sensitivity analysis methods for identifying influential parameters in a problem with a large number of random variables. In *Risk Analysis III*; WIT Press: Southampton, UK, 2002.